

The Changes of Leaf Reflectance Spectrum and Leaf Functional Traits of *Osmanthus Fragrans* are Related to the Parasitism of *Cuscuta Japonica*

Jiyou Zhu

Beijing Forestry University <https://orcid.org/0000-0001-9031-5548>

Qing Xu

Beijing Forestry University

Weijun He

Chinese Academy of Forestry

Jiangming Yao

Guangxi University

Xinna Zhang (✉ zhangxinna0513@163.com)

Beijing Forestry University

Chengyang Xu

Beijing Forestry University

Research article

Keywords: Leaf reflectance spectrum, Leaf functional traits, Leaf economics spectrum, Parasitic, *Cuscuta japonica* Choisy, *Osmanthus fragrans*

Posted Date: December 7th, 2020

DOI: <https://doi.org/10.21203/rs.3.rs-117885/v1>

License: © ⓘ This work is licensed under a Creative Commons Attribution 4.0 International License.

[Read Full License](#)

Abstract

Background: Studies on the influence of parasitism on plants based on hyperspectral analysis have not been reported so far. To fully understand the variation characteristics and laws of leaf reflectance spectrum and functional traits after the urban plant parasitized by *Cuscuta japonica* Choisy. *Osmanthus fragrans* (Thunb.) Lour. was taken as the research object to analyze the spectral reflectance and functional traits characteristics at different parasitismal stages.

Results: Results showed that the spectral reflectance was higher than the parasitic reflectance in the visible light and near infrared. The spectral reflectance in 750 ~ 1400 nm was the sensitive range of spectral response of host plants to parasitic infection, which is universal at different parasitic stages. We established a chlorophyll inversion model ($y = -65913.323x + 9.783$, $R^2 = 0.6888$) based on the reflectance of red valley (minimum band reflectance in the range of 640 ~ 700 nm), which can be used for chlorophyll content of the parasitic *Osmanthus fragrans*. There was a significant correlation between spectral characteristic parameters and chlorophyll content index. Through the change of spectral parameters, we can predict the chlorophyll content of *Osmanthus fragrans* under different parasitism degrees.

Conclusion: After the host plant was invaded by parasitic plants, its leaf functional traits are generally characterized by thick leaf, small leaf area, small specific leaf area, low relative chlorophyll content, high dry matter content and high leaf tissue density. These findings indicate that the host plant have taken certain trade-off strategy to maintain their growth in the environment invaded by parasitic plants. Therefore, we suspect that there may be leaf economics spectrum in the parasitic environment, and there was a general trend toward "slow investment-return" in the global leaf economics spectrum.

Background

The prevalence of plant disease affects agriculture and forestry, reduces the quantity and quality of products, and poses a huge threat to agricultural safety and urban ecology. Parasitic plants are one of the special groups commonly existing in the global ecosystems [2, 3]. The common parasitic plants include Taxillidae, Mistletoe and Cuscutaceae [4, 5]. Among them, Cuscutaceae is one of the most common parasitic plant species in China, and *Cuscuta japonica* Choisy is widely distributed [6]. *Cuscuta chinensis* is seriously short of chlorophyll and other important substances to maintain its photosynthesis due to the degradation of its roots and leaves, commonly known as *Caulis Sinomenii* (6, 7). It usually parasitizes the root and stem of the host plant through its special root absorption, and depends on absorbing carbohydrates, inorganic salts and water from the host to maintain its survival, growth and reproduction [8]. Studies have shown that the host range of *Cuscuta Japonica* Choisy is quite wide, and the vast majority of herbaceous dicotyledonous and monotyledonous plants may become parasitic objects of *Cuscuta japonica* Choisy. *Cuscuta japonica* Choisy usually grows in a winding way and spreads rapidly [9, 10, 11]. In addition, it can quickly form roots and continue to grow after the stem is broken. Moreover, when the damage is serious, the whole host plant is often covered with the stem strips of *Cuscuta japonica* Choisy, causing the host plant to grow poorly and even causing the whole host plant to die [11].

Therefore, parasitic plants are one of the important factors that endanger the urban greening plants and seriously threaten the urban environment. Researches on *Cuscuta japonica Choisy* parasitism mainly focus on its own biological and ecological characteristics and its effects on photosynthetic physiology and ecosystem of parasitic objects [11, 12, 13]. For example, Beifen Yang et al. study the effects of *Cuscuta japonica Choisy* parasitism on the growth and reproduction of *Solidago canadensis* L. Sumin Guo et al. study the growth trade-off mechanism of *Alternanthera philoxeroides* (Mart.) Griseb. on *Cuscuta japonica Choisy* parasitism [14, 15]. All of these indicated that the host plants often change their growth defense strategies to maintain their own survival and reproduction after being subjected to *Cuscuta japonica Choisy* parasitism stress. In addition, many studies have shown that the influence of parasitic plants on the biomass of the community in which they live have many uncertainties, which are often affected by the community's own characteristics, external environment and other factors, and mainly negative effects [16, 17, 18]. *Osmanthus fragrans* Lour., one of the most common tree species in China, plays a major role in the main ecological, cultural and landscape functions of the city. However, the parasitism of *Cuscuta japonica Choisy* seriously hinders the normal growth of *Osmanthus fragrans*. Diagnosis, monitoring and early warning of urban tree health have always been the focus of international urban forestry research. Therefore, how to monitor and obtain the growth status and the infringed status of the damaged vegetation is the key to effectively prevent and control the infringement.

In recent years, with the rapid development of hyperspectral technology, it has been widely used in forestry monitoring. Hyperspectrum has many advantages, such as high resolution, abundant information, simple data acquisition and so on [19, 20]. Different plants have different reflectance spectral characteristics, and the same plant also has different reflectance spectral characteristics under different growth stages and different growth conditions [21, 22]. Such spectral characteristics vary depending on the type of plant, the growth stage, the chlorophyll content, the cell water content, and the health status (whether or not it is affected by diseases, insect pests or parasitic plants) [21, 23, 24]. Plant functional traits refer to a series of internal physiological functions and external morphological characteristics gradually formed during the long-term interaction between plants and environmental factors, thus avoiding and reducing the adverse effects of the environment on them to the greatest extent [25]. In 2004, Wright et al put forward the concept of leaf economics spectrum (LES) for the first time by analyzing the correlation between leaf functional traits. LES is the general internal relationship among functional traits of leaves [26]. The leaf economics spectrum, that is, the intrinsic relationship among leaf functional traits, reflects the resource allocation trade-off strategy among the functional traits [27]. Leaf functional traits can objectively reflect the impact of environmental changes on plants and the adaptability of plants to the environment, and predict plant characteristics [27, 28, 29]. Therefore, we suspect that leaf functional traits can also be used to diagnose the relationship between biological interactions, and applying imaging spectral remote sensing technology to study and utilize the change information of the spectral characteristics of affected plants can provide a reliable basis for large-scale monitoring of the occurrence of diseases and insect pests. Related researches based on forestry hyperspectral mainly focus on plant yield, crop seed vigor, plant diseases, and plant feature extraction

[29, 30, 31, 32, 33, 34]. However, there are few studies on the response of plant leaf functional traits and leaf spectral characteristics to parasitic plant invasion have not been reported.

As plants are endangered by parasitic plants, they will grow poorly or even die within a certain period of time [30, 35, 36]. Therefore, how to monitor and obtain the growth status and the invasion of the damaged vegetation is the key to effectively prevent and control parasitism. In order to fully understand the changing characteristics and laws of leaf spectrum and leaf functional traits of host plants after being parasitized, and to further explore the response mechanism of leaf reflection spectrum and plant traits to plant parasitic stress. In this study, *Osmanthus fragrans* Lour., a typical greening tree species in China, was taken as the research object. Spectral reflectance characteristics and leaf functional traits of *Osmanthus fragrans* leaves before and after being parasitized by *Cuscuta japonica* Choisy and different parasitic areas were analyzed, and sensitive bands of *Osmanthus fragrans* response to parasitic stress were obtained. The results provide a reference for the monitoring and early warning of the parasitism of *Cuscuta japonica* Choisy. At the same time, it provides a new experimental basis for different measures to control *Cuscuta japonica* Choisy and provides a theoretical basis for an in-depth understanding of the parasitic damage mechanism of *Cuscuta japonica* Choisy and its control strategies.

Results

Changes in Leaf Functional Traits of *Osmanthus fragrans* Leaves Parasitized by *Cuscuta japonica* Choisy

In this study, we selected six plant functional traits which are sensitive to environmental changes and external stress, including chlorophyll content, leaf area, leaf thickness, specific leaf area, leaf dry matter content and leaf tissue density. As shown in Fig. 1, there are significant differences in leaf functional traits of *Osmanthus fragrans* between healthy leaves and the leaves being parasitic by *Cuscuta japonica* Choisy. The chlorophyll content index, leaf area and specific leaf area of *Osmanthus fragrans* were significantly lower than those after parasitism, and with the increase of parasitism intensity, these indexes gradually decreased (CK > T1 > T2 > T3). On the contrary, the leaf thickness, dry matter content and leaf tissue density of *Osmanthus fragrans* were significantly higher than those after parasitism, and these indexes gradually increased with the increase of parasitism intensity (CK < T1 < T2 < T3). Studies show that chlorophyll is one of the important pigments in plant photosynthesis. As the increase of parasitic intensity, chlorophyll content index decreases gradually. The reasons may be that the poor growth of *Cuscuta japonica* Choisy due to its foraging of host nutrients, water, and nutrients after parasitization [37, 38, 39]. In addition, the host plant lacks sufficient light due to the overgrowth of the parasitic plant *Cuscuta japonica* Choisy, which results in large area shading [40, 41].

Spectral characteristics of *Osmanthus fragrans* before and after parasitizing by *Cuscuta japonica* Choisy

As shown in Fig. 2, before and after *Cuscuta japonica* Choisy parasitism, the trend changes of spectral reflectance curves of *Osmanthus fragrans* leaves generally tend to be consistent. In the visible to the near-infrared band (350 ~ 1800 nm), the spectral reflectance is obviously different, which generally

showing before parasitism (average value 0.0676 ~ 1.2633) and after parasitism (average value 0.0430 ~ 1.0061), but after parasitism, the spectral reflectance of *Osmanthus fragrans* is slightly higher than that of healthy *Osmanthus fragrans* in the band 350 ~ 750 nm. In addition, in the range of 350 ~ 1800 nm, there are four main reflection peaks and five main absorption valleys in the spectral reflection curve of *Osmanthus fragrans* leaves to all treatments, and their positions are basically the same. The reflection peaks are respectively located at 560 nm, 1150 nm, 1300 nm and 1650 nm, and the absorption valleys are respectively located in the ranges of 350–560 nm, 600–700 nm, 950–1050 nm, 1150 ~ 1250 nm, and 1400 ~ 1500 nm. According to Table 1, chlorophyll content index of *Osmanthus fragrans* gradually decreased with the deepening of parasitism. Previous studies have shown that chlorophyll content can better characterize the light reflection curve of plant leaves [31, 42]. Therefore, the spectral reflectance curve of the parasitized *Osmanthus fragrans* leaves is higher than that of the non-parasitized healthy *Osmanthus fragrans* leaves, which may be related to the decrease of chlorophyll content.

Figure 2 Spectral characteristics of the healthy *Osmanthus fragrans* and the *Osmanthus fragrans* be parasitized with *Cuscuta japonica Choisy*.

Spectral characteristics of *Osmanthus Fragrans* leaves under the different parasitic intensity of *Cuscuta japonica Choisy*

As can be seen from Fig. 3, under different parasitic intensities of *Cuscuta japonica Choisy*, the leaf surface spectral reflectance curves of *Osmanthus fragrans* are basically the same, but the spectral reflectance values are significantly different. Spectral reflectance values generally decreasing with the deepening of parasitic intensity, and the reflectance values are CK > T1 > T2 > T3. In the visible light to near-infrared 350 ~ 1800 nm band, the spectral reflectance of *Osmanthus fragrans* leaves under different parasitic intensities is the most easily distinguished in the range of 750 ~ 1400 nm, which indicated that this band is the sensitive range of host plants' spectral response to parasitic infection, and at the same time, this change characteristic is common under different parasitic conditions. In addition, we can also see that the spectral reflectance curve slope of *Osmanthus fragrans* leaves has a sharp increasing trend in the range of 700 ~ 780 nm. Studies have shown that the phenomenon of plants increasing suddenly in this waveband belongs to the typical "red edge effect" characteristic of plants. At the same time, the spectral reflectance of the leaves of the host plant (*Osmanthus fragrans*) with different relative chlorophyll contents has a higher reflection platform in the range of 750 ~ 1400 nm, which is wavy and may be affected by the cell structure of the leaves [43, 44]. Among them, the sample with the lowest reflection coefficient are the sample with the lowest chlorophyll content index (the highest parasitic intensity). The reflectance of the sample with the highest chlorophyll content (without parasitism) is the highest at 1150 nm, which is 0.998. There is a significant valley at 1350 ~ 1800 nm, which may be closely related to light absorption by water [45, 46, 47, 48].

Dynamic changes of spectral characteristic parameters of *Osmanthus fragrans* in different parasitic stages

From Fig. 4 and Fig. 5, it can be seen that the general trend of the first derivative spectrum of the leaf surface of the host plant under different parasitic intensities from visible light to the near-infrared band (350 ~ 1800 nm) is basically the same, but there are some differences in values. After *Osmanthus fragrans* was parasitized by *Cuscuta japonica Choisy*, there was an obvious "blue shift" in the red edge of its leaf surface spectral curve. With the deepening of parasitic intensity, the degree of "blue shift" also increased, indicating that with the increase of parasitic intensity, the influence on the red edge of the leaf surface became more severe. In addition, the slope of the red edge of the host plant decreased obviously after parasitization (CK > T1 > T2 > T3). Many studies show that the red edge slope has a good indication of chlorophyll content [49]. Combined with Table 1, it can be seen that with the deepening of parasitic intensity, chlorophyll is decreasing. Therefore, we suspect that the cause of this phenomenon may be related to the influence of *Cuscuta japonica Choisy* on the photosynthesis of host plants. Generally speaking, the red valley reflectance of healthy plants is the highest, but with the deepening of parasitic intensity, the spectral red valley reflectance of host plants shows a decreasing trend with T1 > T2 > T3. Under different parasitic conditions, the position of the yellow edge is not affected, and it is all at 570 nm. However, with the deepening of parasitic intensity, the slope of the yellow edge and the reflectivity of the green peak gradually decreases, while the position of the green peak presents shifts to the long wave direction. At this time, the reflectivity of the water stress wave band increases gradually. Studies have shown that the spectral reflectance of vegetation in the range of 1550 ~ 1750 nm is usually closely related to the cell structure and water content of plants, which indicated the water absorption characteristics [50]. Therefore, with the deepening of the invasion degree of *Cuscuta japonica Choisy*, the cell structure of the leaves suffers certain damage, and the cell fluid of the leaves gradually decreases, thus causing the absorption of light to decrease and the reflection to obviously increase.

Correlation between chlorophyll content and spectral characteristic parameters of host plants with different parasitic degree of *Cuscuta japonica Choisy*

As shown in Fig. 1, CCI of the host plant (*Osmanthus fragrans*) gradually decreased with the deepening of the parasitic intensity of *Cuscuta japonica Choisy*. Previous studies generally believed that chlorophyll was an important parameter to determine the spectral reflectance curve characteristics of plant [51]. When the vegetation is in a healthy growth state and the chlorophyll content is high, the position of the red edge moves towards the long wave direction [51, 52]. However, when vegetation is subjected to external environmental stress, such as drought stress, high temperature stress or pest damage, the red edge position tends to the short-wave direction [53]. Figure 6 and Table 1 showed the correlation between different spectral parameters and CCI and LT. The results of correlation analysis between plant functional traits and spectral parameters show that they show different correlations. It can be seen that there was an extremely significant correlation between spectral parameters and CCI. There was a significant correlation between RGP and LT. Among RRV, RGP, RES, RWSB and CCI were all highly correlated. The correlation between valley reflectance and chlorophyll content reaching the maximum ($y = -65913.323x + 9.783$, $R^2 = 0.6888$), which indicated that red edge characteristics were very sensitive to parasitic infestation and can be used to characterize changes in chlorophyll content of *Osmanthus fragrans* under

different parasitic degrees. As shown in Fig. 7, we tested the chlorophyll inversion model of red valley reflectance, and found that the prediction accuracy of this model was high and stable ($R^2 = 0.8811$, RMSE = 0.0004).

Table 1

Pearson correlation analysis between chlorophyll content index and spectral feature parameters. * indicates that the correlation reaches a significant level at the level of $P < 0.05$. and ** indicates a significant correlation between functional traits.

	RRV	RGP	RES	RWSB
LT	0.25218	-0.1787	-0.28318*	0.09577
LA	-0.01651	0.18462	-0.14292	0.0353
LDMC	0.01136	-0.00523	0.03048	0.09512
SLA	0.20281	-0.24112	-0.06407	0.0641
LTD	-0.19553	0.17124	0.13662	-0.01367
CCI	-0.82993**	0.72953**	0.65295**	-0.56967**

Effects of parasitic plants on the correlation of functional traits of *Osmanthus fragrans* and analysis of leaf economics spectrum

As can be seen from Table 2, there was an interdependent relationship between the functional traits of the leaves. There was a significant positive correlation between LA and SLA. There is a significant negative correlation between SLA and LDMC and LTD. LA was significantly negatively correlated with LDMC and LTD. There was a significant negative correlation between LT and LTD. There was a very significant positive correlation between LDMC and LTD. There was a significant positive correlation between CCI and SLA. At the same time, LT has a negative correlation with SLA and LA, but the correlation has not reached a significant level.

Table 2

Correlation between plant functional traits indicators. * indicates a significant correlation between functional traits at the level of $P < 0.05$, and ** indicates a significant correlation between functional traits at the level of $P < 0.01$.

	LT	LA	SLA	LDMC	LTD	CCI
LT	1					
LA	-0.1696	1				
SLA	-0.1502	0.3581*	1			
LDMC	-0.1293	-0.4246*	-0.6991**	1		
LTD	-0.5436**	-0.4218*	-0.5950**	0.7517**	1	
CCI	0.2566	0.2623	0.4993*	-0.2201	-0.4456*	1

Studies have shown that leaf functional traits can reflect the adaptability of plants to the environment, but compared with a single leaf functional trait, continuous leaf economic spectrum can better reflect the growth strategy and adaptation mechanism of plants [54, 55]. In this study, there was an obvious trade-off relationship between the functional traits of plant leaves, which indicated that when plants are damaged by parasitic plants, host plants show certain ecological trade-off strategies in terms of functional traits for survive. SLA is closely related to the growth and survival strategy of plants, and can represent the ability of plants to adapt the environment and obtain resources [56]. In this study, after being invaded by parasitic plants, the reduction of SLA of the host plants makes the plants more adaptable to resource-poor environment. LDMC represents the of plants to maintain nutrients, while LTD reflects the bearing capacity and defense ability of plant leaves, which is closely related to the turnover growth rate of leaves [56, 57]. In this study, LDMC and LTD increased gradually with the increase of parasitic intensity, and showed a very significant positive correlation. This indicates that the plants can improve the nutrient retention ability of leaves under the adverse environment of parasitic stress, thus making more effective use of limited resources. The increase of LTD is beneficial to enhance the defense ability of plants against biological factors. To sum up, after the host plant was invaded by parasitic plants, its leaf functional traits are generally characterized by large leaf thickness, small leaf area, small specific leaf area, low chlorophyll content index, high dry matter content and high leaf tissue density. Therefore, we suspect that the leaf economics spectrum may also exist in the parasitic environment, and there was a general trend toward “slow investment-return” type in the global leaf economics spectrum (Fig. 8).

Conclusion

In this paper, *Osmanthus fragrans* is used as the research object to analyze the spectral characteristics and leaf functional traits of different parasitic periods after the natural infection of *Cuscuta japonica* Choisy, revealing the relationship between the spectral characteristic changes and invasive processes

after host susceptibility, aiming to use the hyperspectral remote sensing technology for parasitization. In addition, by establishing a correlation between spectral characteristic parameters and chlorophyll content, the research results can provide theoretical support for the prediction of plant diseases in the early stage. At the same time, it can provide a reference for monitoring and early warning of infringement, and a new experimental basis for different measures to control *Cuscuta japonica Choisy*. Main conclusions are as follows.

(1) Before and after being parasitized by *Cuscuta japonica Choisy*, the trend of spectral reflectance curve of *Osmanthus fragrans* leaves tend to be consistent in general. The spectral reflectance is obviously different, and it is generally higher before parasitism than after parasitism. In the range of 350 ~ 1800 nm, there are four main reflection peaks and five main absorption valleys in the spectral reflection curve of *Osmanthus fragrans* leaves.

(2) Visible light band was difficult to reflect the harm of host plants, while the near-infrared band (750 ~ 1400 nm) has the greatest degree of spectral reflectance discrimination. This band was the sensitive range of spectral response of host plants to parasitic infection. At the same time, such variation characteristics were universal under different parasitic degree conditions, and can better reflect the harm of host plants.

(3) The position of red edge, the slope of red edge, reflectance of a green peak, and reflectance of water stress band can well reflect the invasion status of *Cuscuta japonica Choisy* in different parasitic stages. After parasitism, the red edge position of the host plant spectrum shifted to shortwave direction. With the deepening of parasitic intensity, the influence on the red edge position becomes more and more serious, and the degree of "short wave migration" also increases. The red edge slope decreased, and the reflectivity of water stress band increased gradually.

(4) With the increase of parasitic intensity, the relative content of chlorophyll in host plants gradually decreases, and the spectral characteristic parameters are significantly correlated with them. Chlorophyll inversion model based on red valley reflectance has the highest accuracy ($y = -65913.323x + 9.783$, $R^2 = 0.6888$), and can be used for chlorophyll content of parasitic *Osmanthus fragrans*.

(5) After the host plant was invaded by parasitic plants, its leaf functional traits are characterized by large leaf thickness, small leaf area, small specific leaf area, low relative chlorophyll content, high dry matter content, and high leaf tissue density. Therefore, we suspect that there may be leaf economics spectrum in the parasitic environment, and there was a general trend toward "slow investment-return" in the global leaf economics spectrum.

Methods

Research area and sample collection

Nanning city is located in the southwest of Guangxi province, between 107°45' -108°51' east longitude and 22°13' -23°32' north latitude. It is a humid subtropical monsoon climate with abundant sunshine and rainfall throughout the year. The annual average temperature is about 21.6°C, the annual average rainfall is 1304.2 mm, and the average relative humidity is 79% (Quoted from <https://baike.baidu.com>). The sampling area is located on the campuses of Guangxi University, Guangxi Finance and Economics University, and Guangxi Nationalities University. The straight distance of the three locations is about 8 km, and they all belong to community-based environments, ensuring the relative consistency of atmosphere, planting and maintenance management conditions. According to the proportion of the parasitic area of *Cuscuta japonica* Choisy to the crown area of the host plant, it is divided into four parasitic degrees (CK—Without parasitic, T1—Initial parasitism: less than 50%, T2—Parasitic metaphase: 50% ~ 80%, T3—Late parasitism: more than 80%), 30 *Osmanthus fragrans* of 15 ~ 20 years old and healthy growth per treatment were selected, and the planting location was away from the influence of tall buildings and tall trees. Leaf samples were collected from 10: 00 a.m. to 12: 00 a.m. on June 2019. Ten mature and healthy leaves were cut from each tree, placed in an icebox and immediately brought back to the laboratory for spectral determination. The time from leaves collection to spectral measurement is controlled within 15 min, thus ensuring the original growth activity of leaf samples. As shown in Fig. 9, Fig. 9(a) is a plant that is not parasitic and Fig. 9(b) is a plant that is parasitic by *Cuscuta japonica* Choisy. Professor Wei Jiguang from Agricultural College of Guangxi University identified the plants and plant diseases involved in this study.

Leaf reflectance spectrum collection and calculation method of leaf functional traits

FieldSpec3 near-infrared spectrometer (ASD, Malvern Panalytical, USA) was used to collect spectral data. The spectrum band acquired by this instrument ranges from 300 nm to 2500 nm. The final output spectral reflectance curve is the average of 10 repetitions. The spectral measurement process is shown in Fig. 2. The light source is the solar light source during 12: 00 to 13: 00. Whiteboard is manufactured from a sintered polytetrafluoroethylene (PTFE) based material. In order to reduce human interference, instrument operators wear cotton work clothes.

In July 2019, thirty *Osmanthus fragrans* with different degrees of damage were selected at each test site, and thirty mature and healthy leaves were randomly collected from each plant during 9:00–12:00 in fine weather. The relative chlorophyll content index (CCI) was determined by CCM-200 plus chlorophyll meter (OPTI-Science, Massachusetts, USA). This instrument is recalibrated every 15 minutes. The leaf fresh weight (LFW, g) was weighed using FA/JA electronic balance (Changzhou Xingyun Electronic Equipment Co., Ltd., Changzhou, China). Leaf thickness (LT, mm) was measured by CD-15AX caliper rule (Mitutoyo, Shanghai, China). The leaf area (LA, cm²) was measured by a DS-310/360W scanner (Epson (china) co., ltd, Beijing, China), then placed in 9030A Electric constant temperature blast dry box (Yiheng, Shanghai, China) at 60 °C, the leaf dry weight (LDW, g) was weighed by FA/JA electronic balance. Specific leaf area

(SLA, m²/g) = LA/LDW. Leaf volume (LV, cm³) = LT × LA. Leaf tissue density (LTD, g/cm³) =LDW/LV. Leaf dry matter content (LDMC, g/g) = LDW/LFW.

As shown in Table 1, the hyperspectral characteristic parameters selected in this study include the position of red edge (REP), the slope of red edge (RES), the reflectance of red valley (RRV), the reflectance of green peak (RGP), the position of green peak (GPP), the reflectance of water stress band (RWSB), the slope of yellow edge (YES), and the position of yellow edge [58, 59, 60].

Table 3
Spectral parameters and their description.

Spectral parameter	Description
RES	The maximum reflectance in the red band (680 ~ 750 nm).
REP	The wavelength position corresponding to the maximum reflectance in the wavelength band 680 ~ 750 nm.
RRV	Minimum band reflectance in the range of 640 ~ 700 nm.
RGP	Maximum band reflectance in the range of 510 ~ 580 nm.
GPP	The wavelength position corresponding to the green peak reflectance in the wavelength band 510 ~ 580 nm.
RWSB	Maximum band reflectance in the range of wavelengths from 1550 ~ 1750 nm.
YES	The maximum reflectance in the yellow band (550–582 nm).
YEP	The wavelength position corresponding to the maximum reflectance in the wavelength band 550 ~ 582 nm.

Abbreviations

SLA-Specific leaf area, LDMC-Leaf dry matter content, CCI-Chlorophyll content index, LTD-Leaf tissue density, LT-Leaf thickness, LSFW-Leaf saturated fresh weight, LV-Leaf volume, LDW- Leaf dry weight, REP-Position of red edge, RES-Slope of red edge, RRV-Reflectance of red valley, RGP-Reflectance of green peak, GPP-Position of green peak, RWSB-Reflectance of water stress band, YES-Slope of yellow edge, YEP-Position of yellow edge.

Declarations

Funding

This study was funded by “the Fundamental Research Funds for the Central Universities (NO. BLX201704)” and “National Natural Science Foundation of China (NSFC project NO.31901277)”.

Acknowledgments

Research was conducted in Guangxi University. We thank the Forestry College of Guangxi University and the Agricultural College of Guangxi University for providing us with necessary experimental platforms and instruments. The English in this document has been checked by at least two professional editors; both were native speakers of English. We thank Professor Jiguang Wei from the College of Agriculture of Guangxi University for identifying the plant species used in this study (Identification information refers to Flora of China).

Authors' contributions

J.Z. conceived and designed the study. J.Z. and X.Z. contributed materials and tools. J.Z., W.H. and Q.X. performed the experiments. J.Y., X.Z. and C.X. contributed to literature collection. J.Z. and W.H. contributed to data analysis. J.Z. and Q.X. contributed to paper preparation, writing and revision. All the authors read and approved it for publication.

Availability of data and materials

The data involved in the article were all shown in the figures and tables. However, there are still available from the first author on reasonable request.

Ethics approval and consent to participate

This experiment does not involve human experiments and animal experiments. The field trial experiments in the current study were permitted by the local government in China (Guangxi University and Guangxi Finance and Economics University), including the collection of leaf samples.

Consent for publication

Not Applicable.

Competing interests

The authors declare that they have no competing interests.

Author details

¹ Research Center for Urban Forestry, Key Laboratory for Silviculture and Conservation of Ministry of Education, Key Laboratory for Silviculture and Forest Ecosystem of State Forestry Administration, Beijing Forestry University, Beijing 100083, China. ² Guangxi University, Nanning 530005, China. ³ Chinese Academy of Forestry, Research Institute of Tropical Forestry, Guangzhou 510520, Guangdong, China.

References

1. Mahlein AK, Oerke EC, Steiner U, Dehne HW. Recent advances in sensing plant diseases for precision crop protection. *Eur J Plant Pathol.* 2012;133(1):197–209.

2. Press MC, Phoenix GK. Impacts of parasitic plants on natural communities. *New Phytol.* 2010;166:737–51.
3. Bouwmeester HJ, Roux C, Lopezraez JA, Bécard G. Rhizosphere communication of plants, parasitic plants and am fungi. *Trends Plant Sci.* 2007;12:224–30.
4. Runyon JB, Mescher MC, Moraes CMD. Volatile chemical cues guide host location and host selection by parasitic plants. *Science.* 2006;313:1964–7.
5. Yoneyama K, Xie X, Sekimoto H, Takeuchi Y, Ogasawara S, Akiyama K, Hayashi H, Yoneyama K. Strigolactones, host recognition signals for root parasitic plants and arbuscular mycorrhizal fungi, from Fabaceae plants. *New phytol.* 2008;179:484–94.
6. Yoneyama K. Studies on the host recognition mechanism of root parasitic plants. *Journal of Pesticide Science.* 2010;35:348–50.
7. Smith JL, De Moraes CM, Mescher MC. Jasmonate- and salicylate-mediated plant defense responses to insect herbivores, pathogens and parasitic plants. *Pest Manag Sci.* 2010;65:497–503.
8. Bardgett RD, Smith RS, Shiel RS, Peacock S, Simkin JM, Quirk H, Hobbs PJ. Parasitic plants indirectly regulate below-ground properties in grassland ecosystems. *Nature.* 2009;439:969–72.
9. Mower JP, Stefanovi CS, Young GJ, Palmer JD. Plant genetics, gene transfer from parasitic to host plants. *Nature.* 2004;432:165–6.
10. Matvienko M, Wojtowicz A, Wrobel R, Jamison D, Goldwasser Y, Yoder JI. Quinone oxidoreductase message levels are differentially regulated in parasitic and non-parasitic plants exposed to allelopathic quinones. *Plant J.* 2010;25:375–87.
11. Pickett JA, Hamilton ML, Hooper AM, Khan ZR, Midega CAO. Companion cropping to manage parasitic plants. *Annual Rev Phytopathol.* 2010;48:161–77.
12. Rubiales D. 2010. Parasitic plants, wild relatives and the nature of resistance. *New Phytol.* 2010;160:459–461.
13. Mahlein A-K, Kuska MT, Behmann J, Polder G, Walter A. Hyperspectral Sensors and Imaging Technologies in Phytopathology: State of the Art. *Annu Rev Phytopathol.* 2018;56:535–58.
14. Kubo M, Ueda H, Park P, Kawaguchi M, Sugimoto Y. Reactions of lotus japonicus ecotypes and mutants to root parasitic plants. *J Plant Physiol.* 2009;166:353–62.
15. Conn CE, Bythell–Douglas R, Neumann D, Yoshida S, Whittington B, Westwood JH, Shirasu K, Bond CS, Dyer KA, Nelson DC. Plant evolution. convergent evolution of strigolactone perception enabled host detection in parasitic plants. *Science.* 2015;349:540–3.
16. Press MC. Carbon acquisition and assimilation in parasitic plants. *Funct Ecol.* 2015;5:278.
17. Roney JK, Khatibi PA, Westwood JH. Cross-species translocation of mRNA from host plants into the parasitic plant dodder. *Plant Physiol.* 2007;143:1037–43.
18. Hautier Y, Hector A, Vojtech E, Purves D, Turnbull LA. (2010) Modelling the growth of parasitic plants. *J Ecol.* 2010;98: 857–866.

19. Chin JA, Wang EC, Kibbe MR. (2001) Evaluation of hyperspectral technology for assessing the presence and severity of peripheral artery disease. *J Vasc Surg* 2001;54: 1679–1688.
20. Xie X, Ying XL, Li R, Zhang Y, Huo Y, Bao Y, Shen S. Hyperspectral characteristics and growth monitoring of rice *Oryza sativa* under asymmetric warming. *Int J Remote Sens.* 2013;34:8449–62.
21. Cuevas P. Effects of generalist and specialist parasitic plants (*Loranthaceae*) on the fluctuating asymmetry patterns of ruprestrian host plants. *Basic Appl Ecol.* 2011;12:449–55.
22. Cavender-Bares J, Meireles JE, Couture JJ, Kaproth MA, Kingdon CC, Singh A, Serbin SP, Center A, Zuniga E, Pilz G, Townsend PA. Associations of leaf spectra with genetic and phylogenetic variation in oaks: Prospects for remote detection of biodiversity. *Remote Sens.* 2016;8.
23. Thenkabail PS, Smith RB, Pauw ED. Hyperspectral vegetation indices and their relationships with agricultural crop characteristics. *Remote Sens Environ.* 2000;71:158–82.
24. Ge S, Everitt J, Carruthers R, Gong P, Anderson G. Hyperspectral characteristics of canopy components and structure for phenological assessment of an invasive weed. *Environ Monit Assess.* 2006;120:109–26.
25. Diaz S, Cabido M, Zak M, Martinez CE, Aranibar J. Plant functional traits, ecosystem structure and land–use history along a climatic gradient in central–western Argentina. *J Veg Sci.* 2010;10:651–60.
26. Wright IJ, Reich PB, Westoby M, Ackerly DD, Baruch Z, Bongers F, Cavender–Bares J, Chapin T, Cornelissen JHC, Diemer M, Flexas J, Garnier E, Groom PK, Gulias J, Hikosaka K, Lamont BB, Lee T, Lee W, Lusk C, Midgley JJ, Navas ML, Niinemets U, Oleksyn J, Osada N, Poorter H, Poot P, Prior L, Pyankov VI, Roumet C, Thomas SC, Tjoelker MG, Veneklaas EJ, Villar R. The worldwide leaf economics spectrum. *Nature.* 2004;428:821–7.
27. Vendramini F, Diaz S, Gurvich DE, Wilson PJ, Thompson K, Hodgson JG. Leaf traits as indicators of resource–use strategy in floras with succulent species. *New Phytol.* 2002;154:147–57.
28. Cornwell WK, Cornelissen JH. Plant species traits are the predominant control on litter decomposition rates within biomes worldwide. *Ecol Lett.* 2008;11:1065–71.
29. Cochrane A, Hoyle GL, Yates CJ, Wood J, Nicotra AB. The phenotypic response of co–occurring banksia species to warming and drying. *Plant Ecol.* 2015;216:27–39.
30. Cheng GF, Zhang JH, Li BB, Zhang JH, Yang SB, Xie XJ. Hyper–Spectral and Red Edge Characteristics for Rice Under Different Temperature Stress Levels. *Jiangsu J Agri Sci.* 2008;5:573–80. (in Chinese).
31. Huang XY, Xu ZH, Lin L, Shi WC, Yu KY, Liu J, Chen CC, Zhou HK. *Pantana Phyllostachysae* Chao damage detection based on physical and chemical parameters of *Moso Bamboo* leaves. *Spectrosc Spect Anal.* 2019;39:857–64.
32. Kim SR, Lee WK, Lim CH, Kim M, Kafatos MC, Lee SH, Lee SS. Hyperspectral analysis of pine wilt disease to determine an optimal detection Index. *Forests.* 2018;9:115.
33. Zhang SL, Qin J, Tang XD, Wang YJ, Huang JL, Song QL, Min JY. Spectral characteristics and evaluation model of *Pinus Massoniana* suffering from *Bursaphelenchus Xylophilus* disease. *Spectrosc Spect Anal.* 2019;39:865–72.

34. Beth F, Anna Y, Cathleen L, Isabella A, Jennifer J, Montgomery RA, Jeannine CB. Spectral differentiation of oak wilt from foliar fungal disease and drought is correlated with physiological changes. *Tree Physiol.* 2020;3.
35. Wright SJ. Leaf functional traits of tropical forest plants in relation to growth form. *Funct Ecol.* 2010;21:19–27.
36. Wickett NJ, Honaas LA, Wafula EK, Das M, Huang K, Wu B, Landherr L, Timko MP, Yoder John., Westwood JH, de Pamphilis CW. Transcriptomes of the parasitic plant family *Orobanchaceae* reveal surprising conservation of chlorophyll synthesis. *Curr Biol.* 2011;21:2098–104.
37. Corney HJ, Sasse JM, Ades PK. Assessment of salt tolerance in eucalypts using chlorophyll fluorescence attributes. *New Forest.* 2003;26:233–46.
38. Dodds KJ, Cooke RR, Hanavan RP. The effects of silvicultural treatment on siren noctilio attacks and tree health in northeastern United States. *Forests.* 2014;5:2810–24.
39. Lu N, Zhou X, Cui M, Yu M, Zhou JX, Qin YS, Li Y. Colonization with arbuscular mycorrhizal fungi promotes the growth of *Morus alba* L. seedlings under greenhouse conditions. *Forests.* 2015;6:734–47.
40. Hegenauer V, Körner M, Albert M. Plants under stress by parasitic plants. *Curr Opin Plant Biol.* 2017;38:34.
41. Zhao XJ, Pan YJ, Chen HF, Tang ZH. Influence of holoparasitic plant *Cuscuta japonica* on growth and alkaloid content of its host shrub *Catharanthus roseus*, a field experiment. *Arab J Sci Eng.* 2018;43:1–8.
42. Reynolds GJ, Gordon TR, McRoberts N. Quantifying the impacts of systemic acquired resistance to pitch canker on Monterey pine growth rate and hyperspectral reflectance. *Forests.* 2016;7:20.
43. Westwood JH, Bouwmeester H. Parasitic plants tap into the main stream. *New Phytol.* 2010;184:284–7.
44. Johnson BI, De Moraes CM, Mescher MC. Manipulation of light spectral quality disrupts host location and attachment by parasitic plants in the genus *Cuscuta*. *J Appl Ecol.* 2016;53:794–803.
45. Kuijt J. Botanical enigmas. (book reviews, the biology of parasitic flowering plants). *Science.* 1970;168:1081–2.
46. Filella I, Penuelas J. The red edge position and shape as indicators of plant chlorophyll content, biomass and hydric status. *Int J Remote Sens.* 1994;15:1459–70.
47. Record S. A World of Opportunists, the Parasitic Plants. *Ecology.* 90: 857–858.
48. Yoneyama K, Awad AA, Xie X, Takeuchi Y. Strigolactones as germination stimulants for root parasitic plants. *Plant Cell Physiol.* 2010;51:1095–103.
49. Han L. Estimating chlorophyll-a concentration using first-derivative spectra in coastal water. *Int J Remote Sens.* 2005;26:5235–44.
50. Jiang J, Steven MD, He R, Chen Y, Du P, Guo H. Identifying the spectral responses of several plant species under CO₂ leakage and waterlogging stresses. *Int J Greenh Gas Con.* 2015;37:1–11.

51. Liu W, Chang QR, Guo M, Xing DX, Yuan YS. Extraction of first derivative spectrum features of soil organic matter via wavelet denoising. *Spectrosc Spect Anal.* 2011;31:100–4.
52. Liu L, Wang J, Huang W, Zhao C, Zhang B, Tong Q. (2003) Estimating winter wheat plant water content using red edge parameters. *Int J Remote Sens.* 2003;25: 1688–1691.
53. Wang ZH, Ding LX. Tree species discrimination based on leaf-level hyperspectral characteristic analysis. *Spectrosc Spect Anal.* 2010;30:1825–9.
54. Atkinson LJ, Campbell CD, Zaragoza-Castells J, Hurry V, Atkin OK. Impact of growth temperature on scaling relationships linking photosynthetic metabolism to leaf functional traits. *Funct Ecol.* 2010;24:1181–91.
55. Ülo N. Leaf age dependent changes in within–canopy variation in leaf functional traits, a meta-analysis. *J Plant Res.* 2016;129:313–38.
56. Lemoine NP, Shue J, Verrico B, Erickson D, Kress WJ, Parker JD. Phylogenetic relatedness and leaf functional traits, not introduced status, influence community assembly. *Ecology.* 2016;96:2605–12.
57. López-sampson A, Cernusak LA, Page T. Relationship between leaf functional traits and productivity in *Aquilaria crassna* (*Thymelaeaceae*) plantations, a tool to aid in the early selection of high–yielding trees. *Tree Physiol.* 2017;37:1–9.
58. Gitelson AA, Merzlyak MN, Lichtenthaler HK. Detection of red edge position and chlorophyll content by reflectance measurements near 700 nm. *J Plant Physiol.* 1996;148:501–8.
59. Cho MA, Skidmore AK. (2006) A new technique for extracting the red edge position from hyperspectral data, the linear extrapolation method. *Remote Sens Environ.* 2006;101: 181–193.
60. Zhu J, Yu Q, Zhu H, He W, Xu C, Liao J, Qiu Y, Su K. Response of dust particle pollution and construction of a leaf dust deposition prediction model based on leaf reflection spectrum characteristics. *Environ Sci Pollut Res.* 2019.

Figures

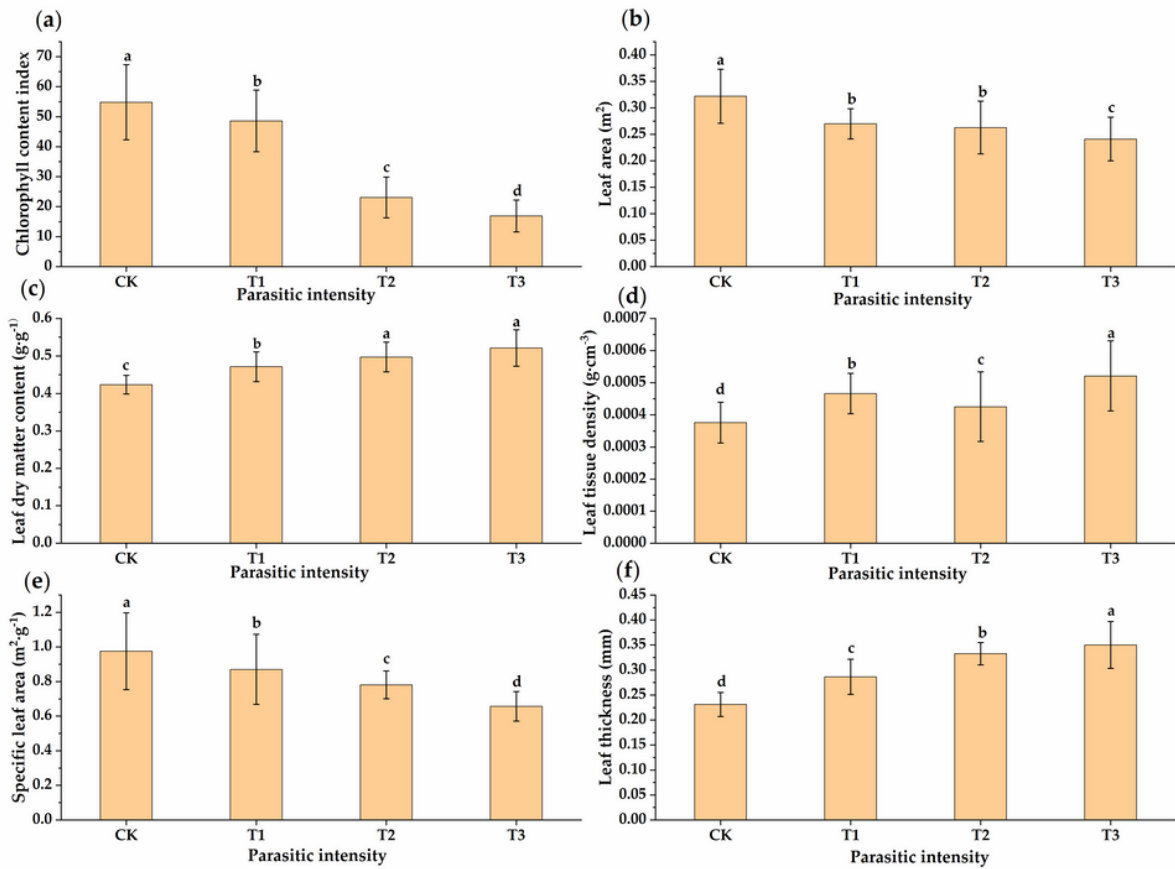


Figure 1

Changes in leaf functional traits under different parasitic intensities. Different lowercase letters indicate significant differences in parameters at the P<0.05 level. (a) Chlorophyll content index, (b) leaf area, (c) leaf dry matter content, (d) leaf tissue density, (e) specific leaf area, (f) leaf thickness

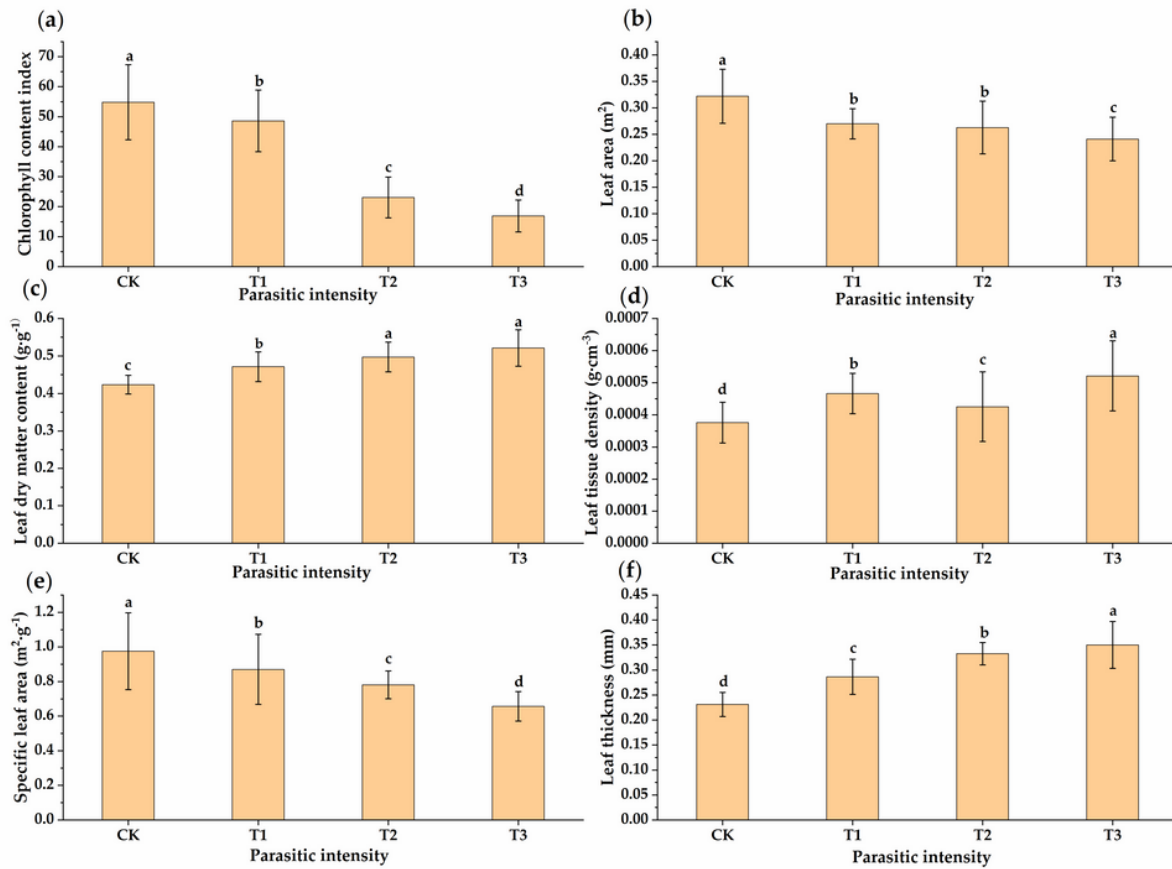


Figure 1

Changes in leaf functional traits under different parasitic intensities. Different lowercase letters indicate significant differences in parameters at the $P < 0.05$ level. (a) Chlorophyll content index, (b) leaf area, (c) leaf dry matter content, (d) leaf tissue density, (e) specific leaf area, (f) leaf thickness

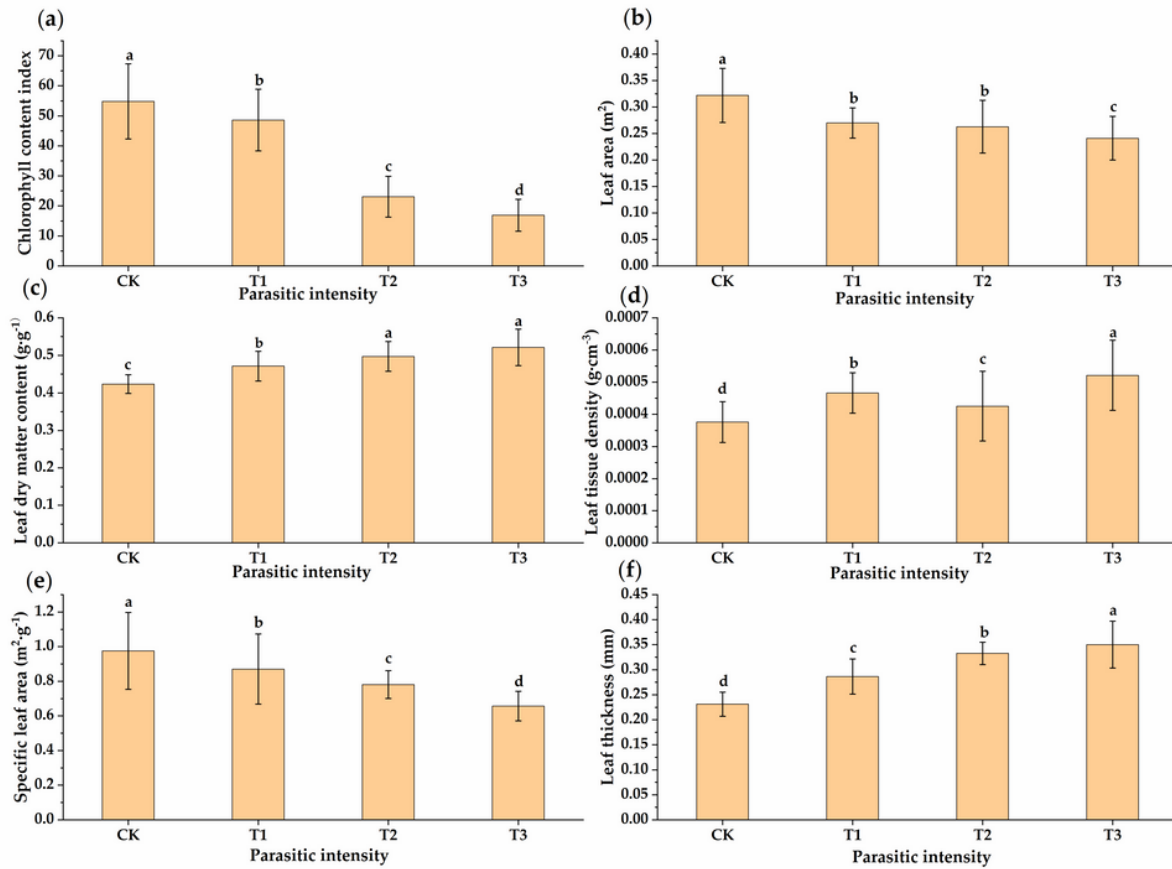


Figure 1

Changes in leaf functional traits under different parasitic intensities. Different lowercase letters indicate significant differences in parameters at the P<0.05 level. (a) Chlorophyll content index, (b) leaf area, (c) leaf dry matter content, (d) leaf tissue density, (e) specific leaf area, (f) leaf thickness

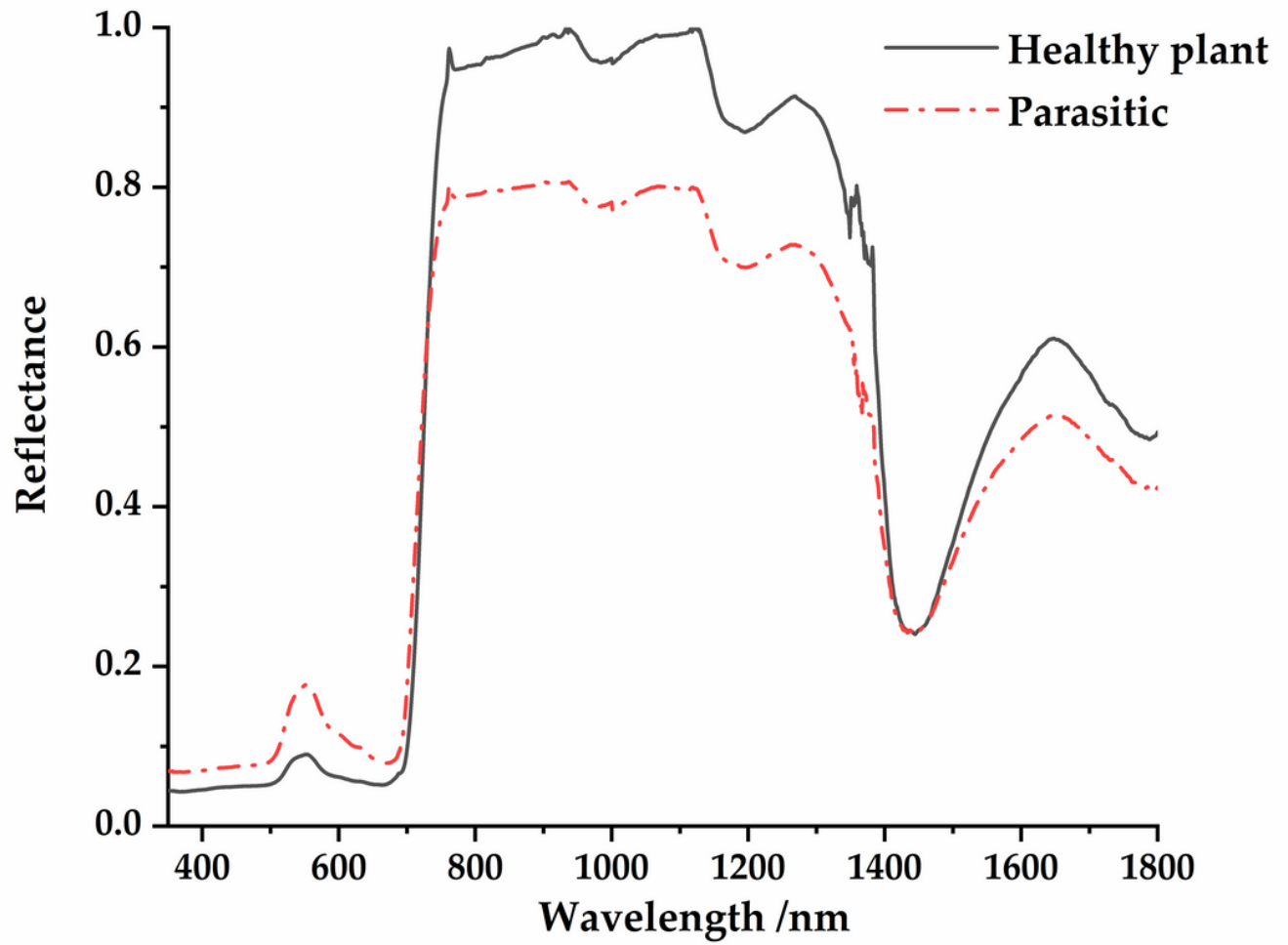


Figure 2

Spectral characteristics of the healthy *Osmanthus fragrans* and the *Osmanthus fragrans* be parasitized with *Cuscuta japonica* Choisy.

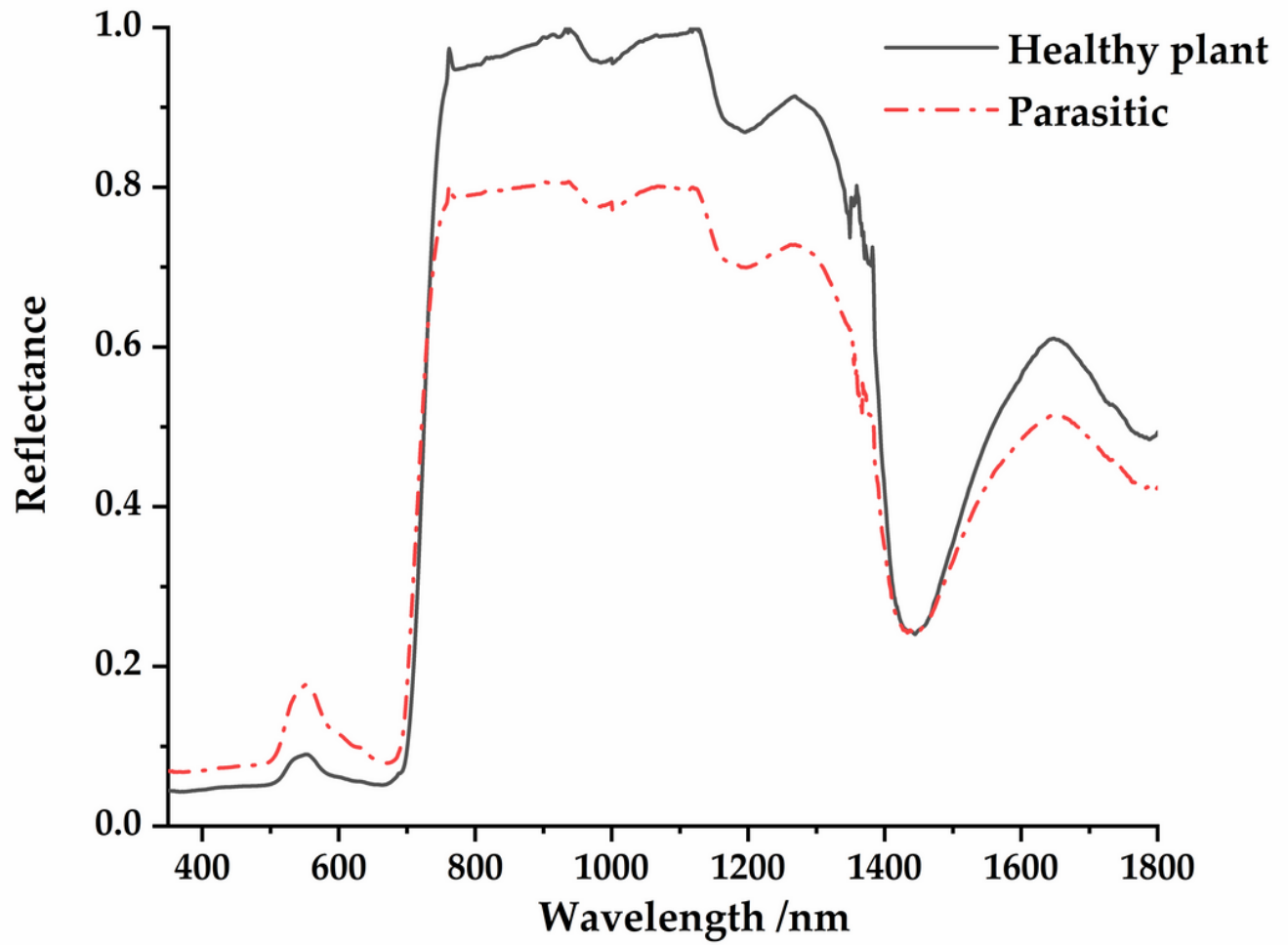


Figure 2

Spectral characteristics of the healthy *Osmanthus fragrans* and the *Osmanthus fragrans* be parasitized with *Cuscuta japonica* Choisy.

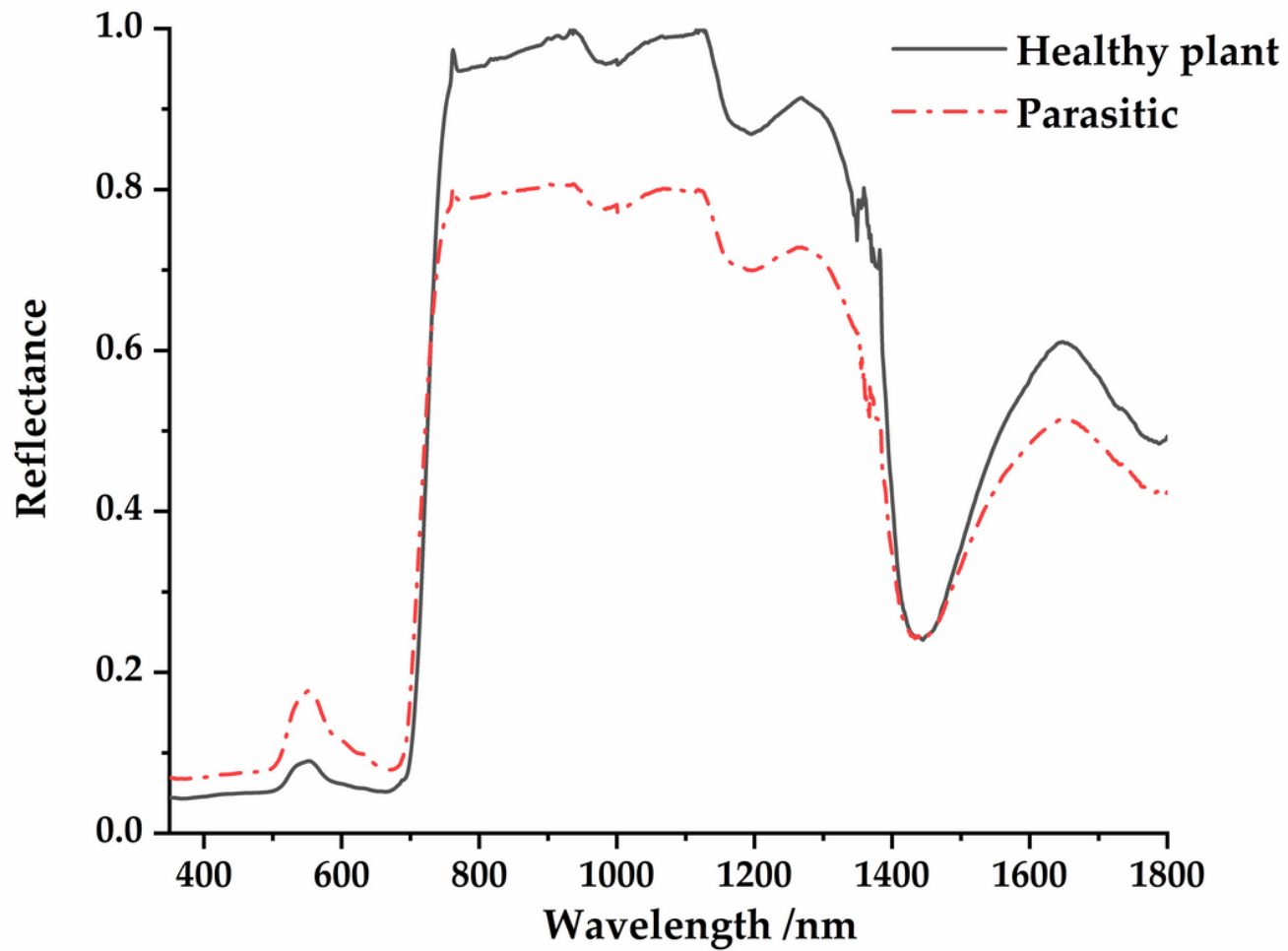


Figure 2

Spectral characteristics of the healthy *Osmanthus fragrans* and the *Osmanthus fragrans* be parasitized with *Cuscuta japonica* Choisy.

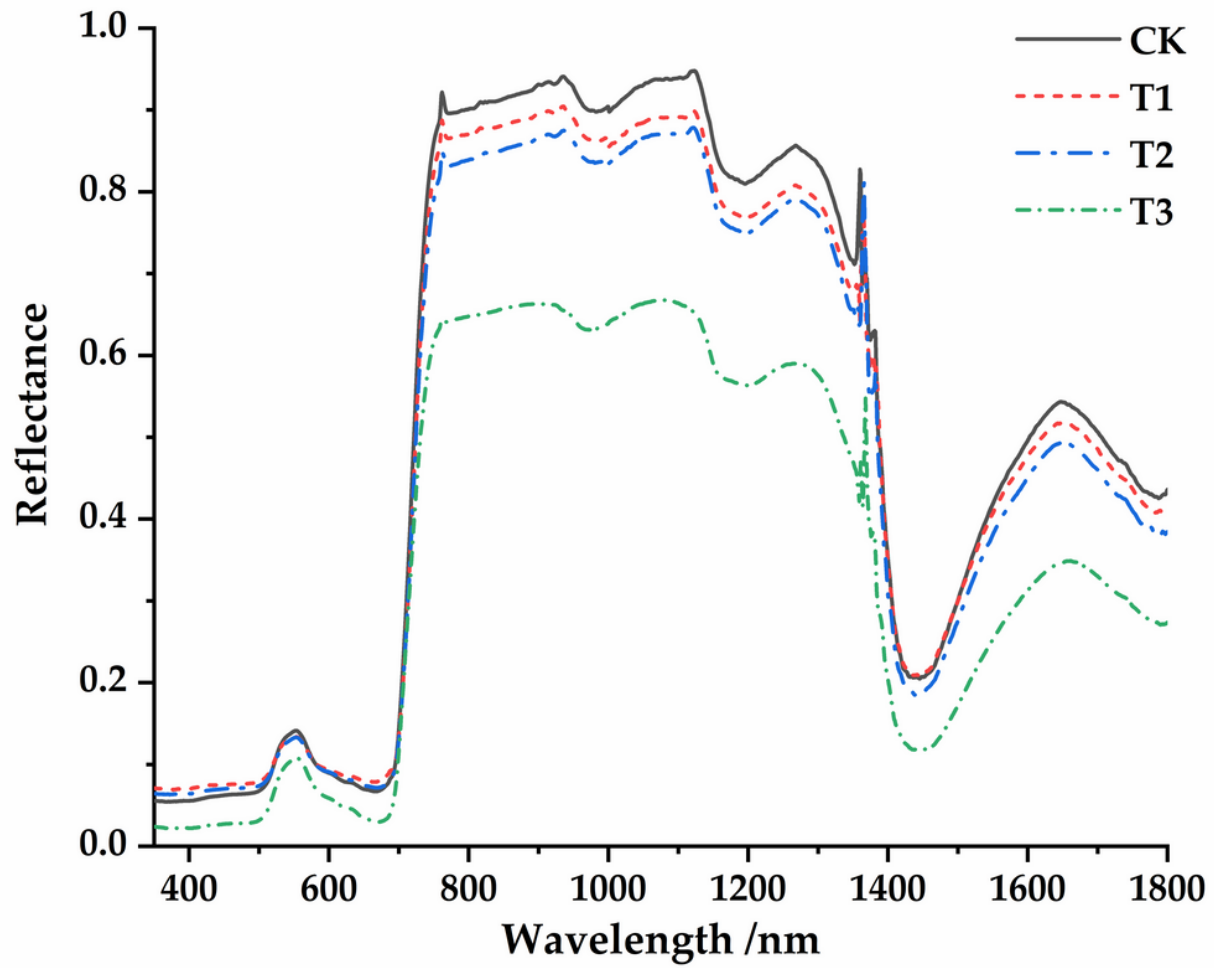


Figure 3

The leaf reflectance spectral curves in different degrees of parasitism.

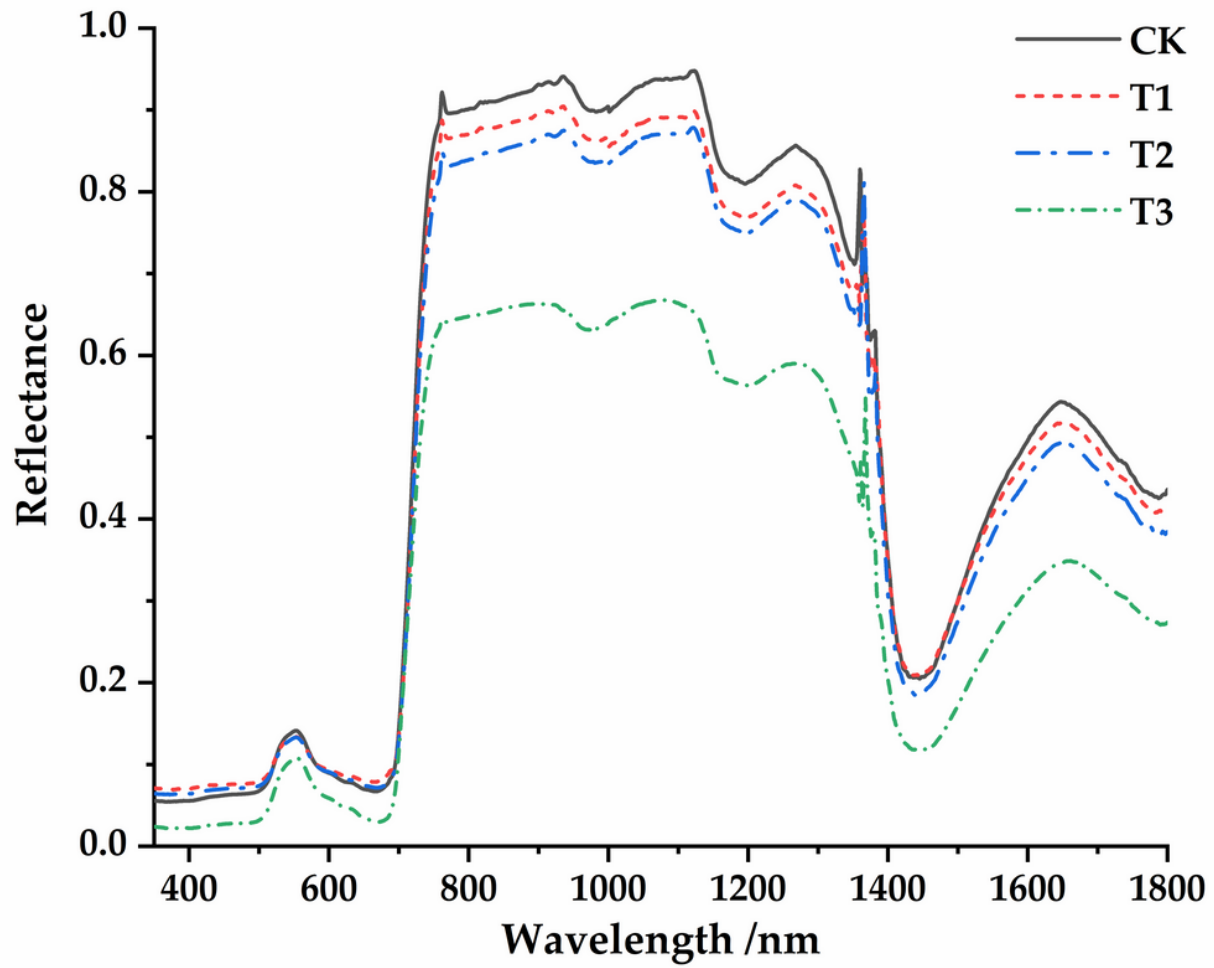


Figure 3

The leaf reflectance spectral curves in different degrees of parasitism.

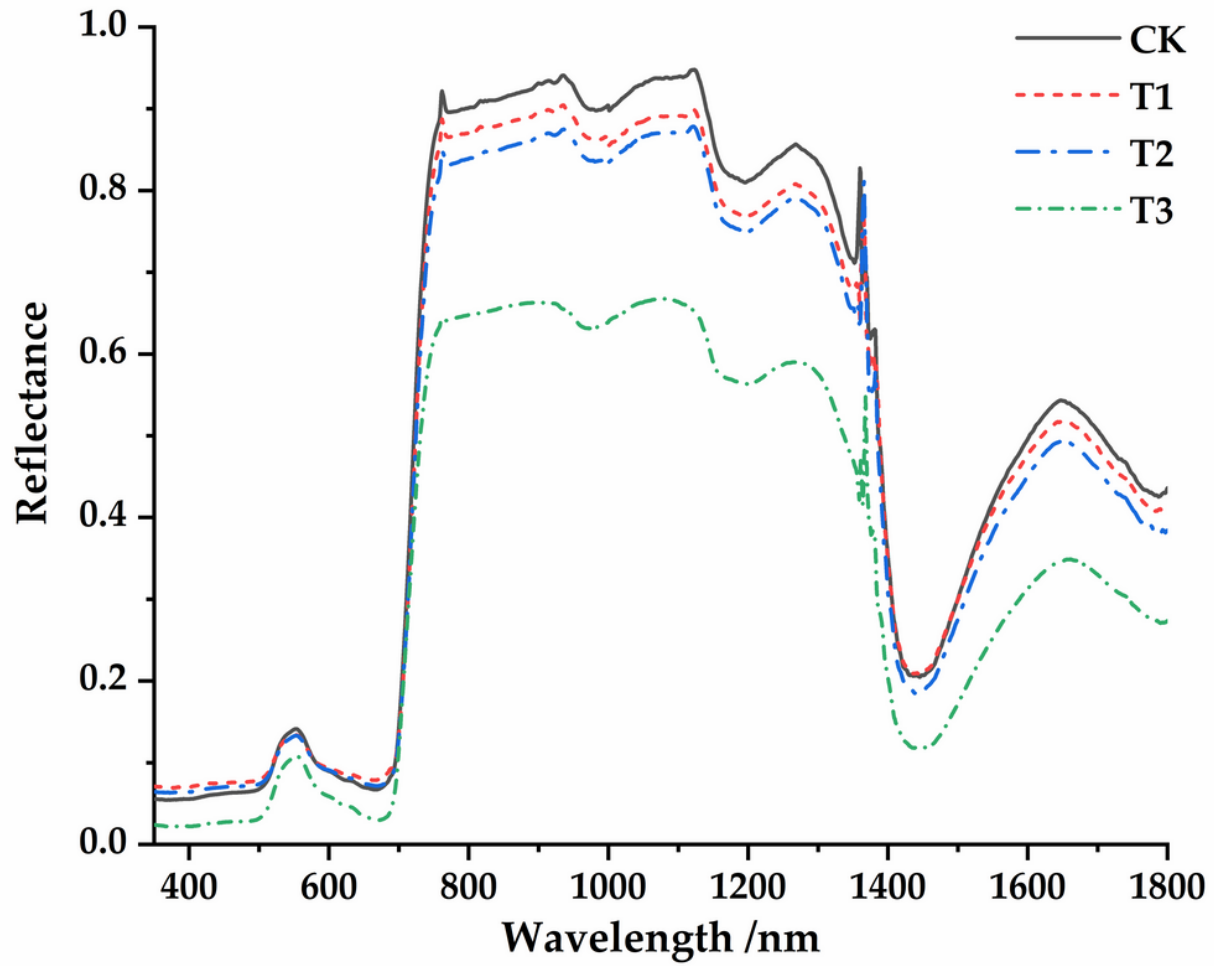


Figure 3

The leaf reflectance spectral curves in different degrees of parasitism.

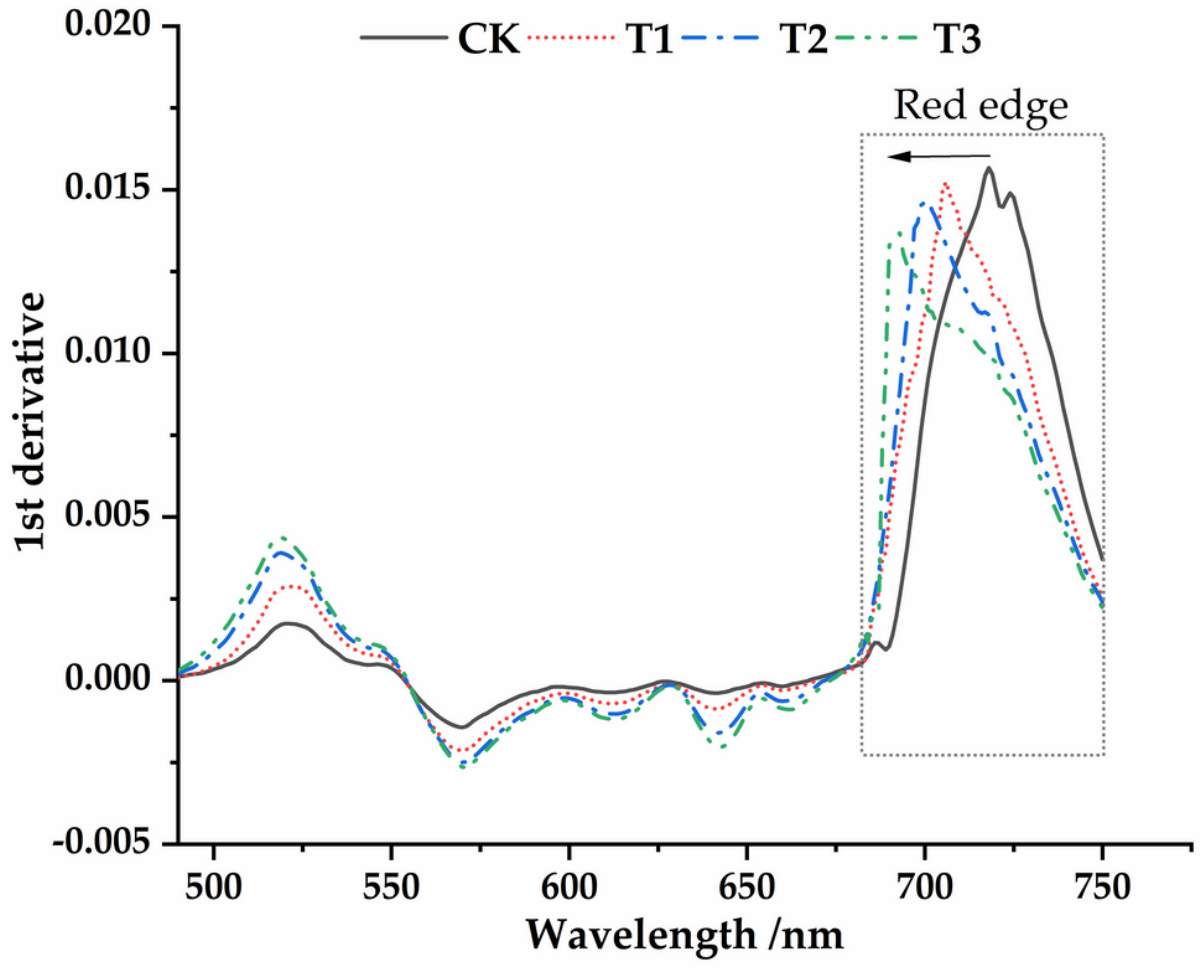


Figure 4

The first derivative spectral curves of the *Osmanthus fragrans* leaves.

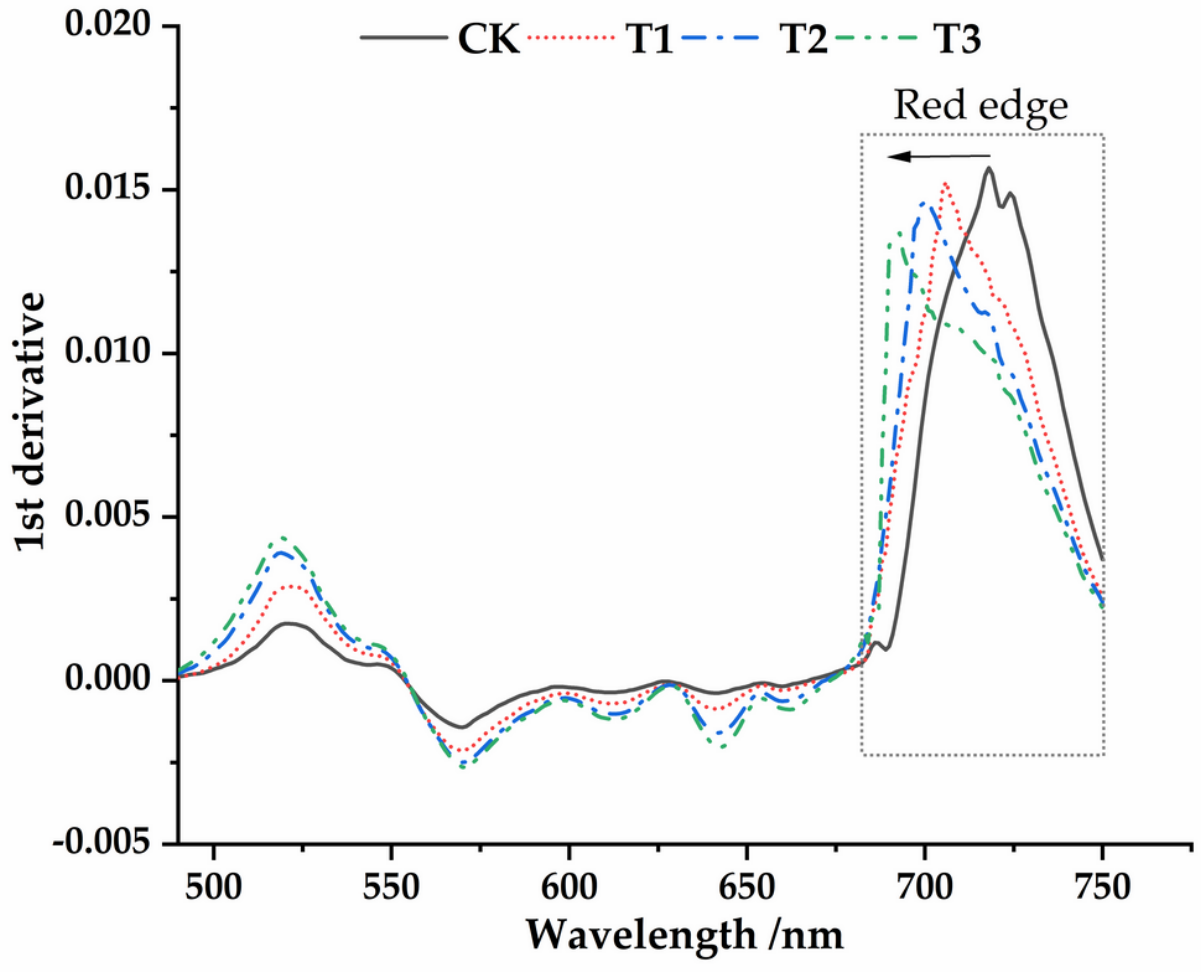


Figure 4

The first derivative spectral curves of the *Osmanthus fragrans* leaves.

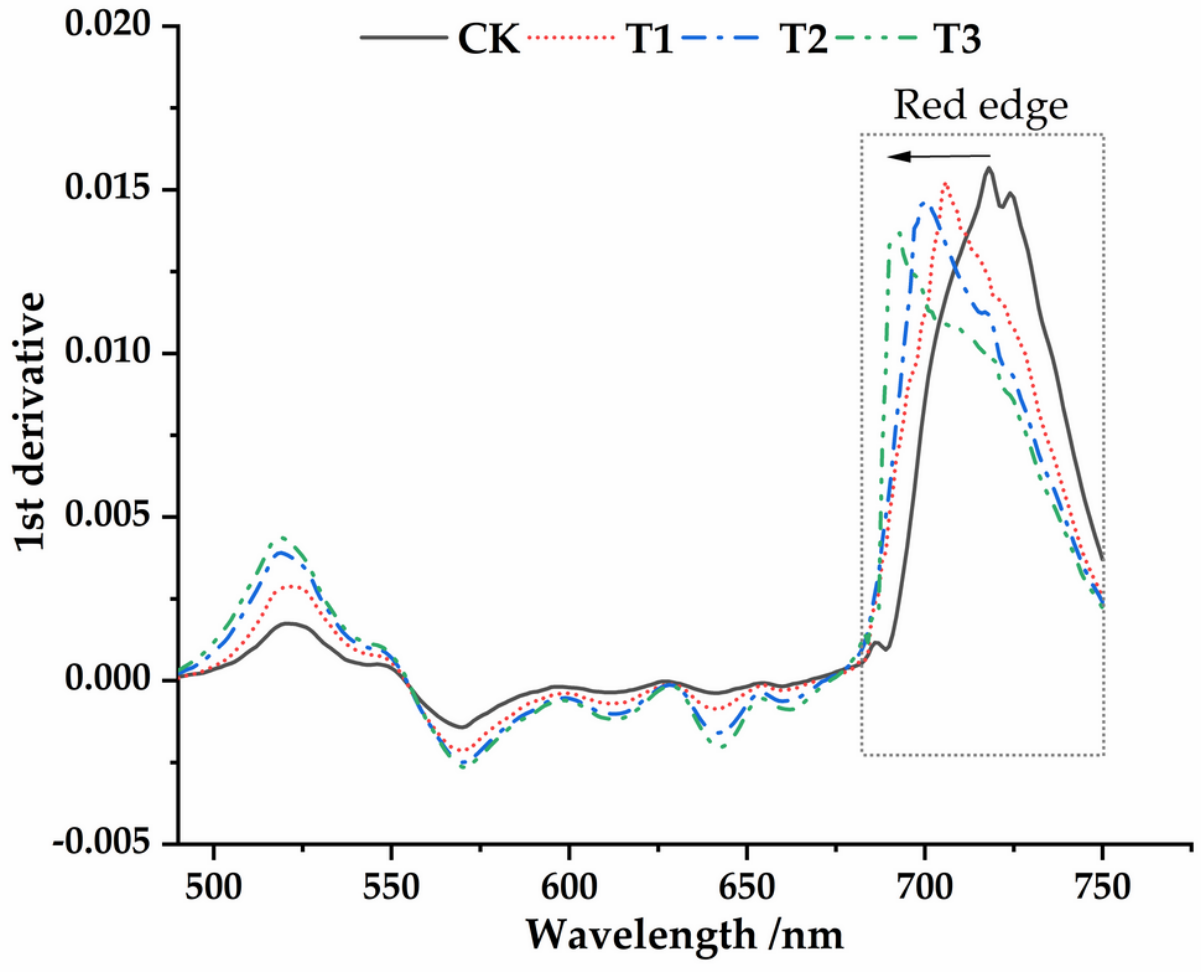


Figure 4

The first derivative spectral curves of the *Osmanthus fragrans* leaves.

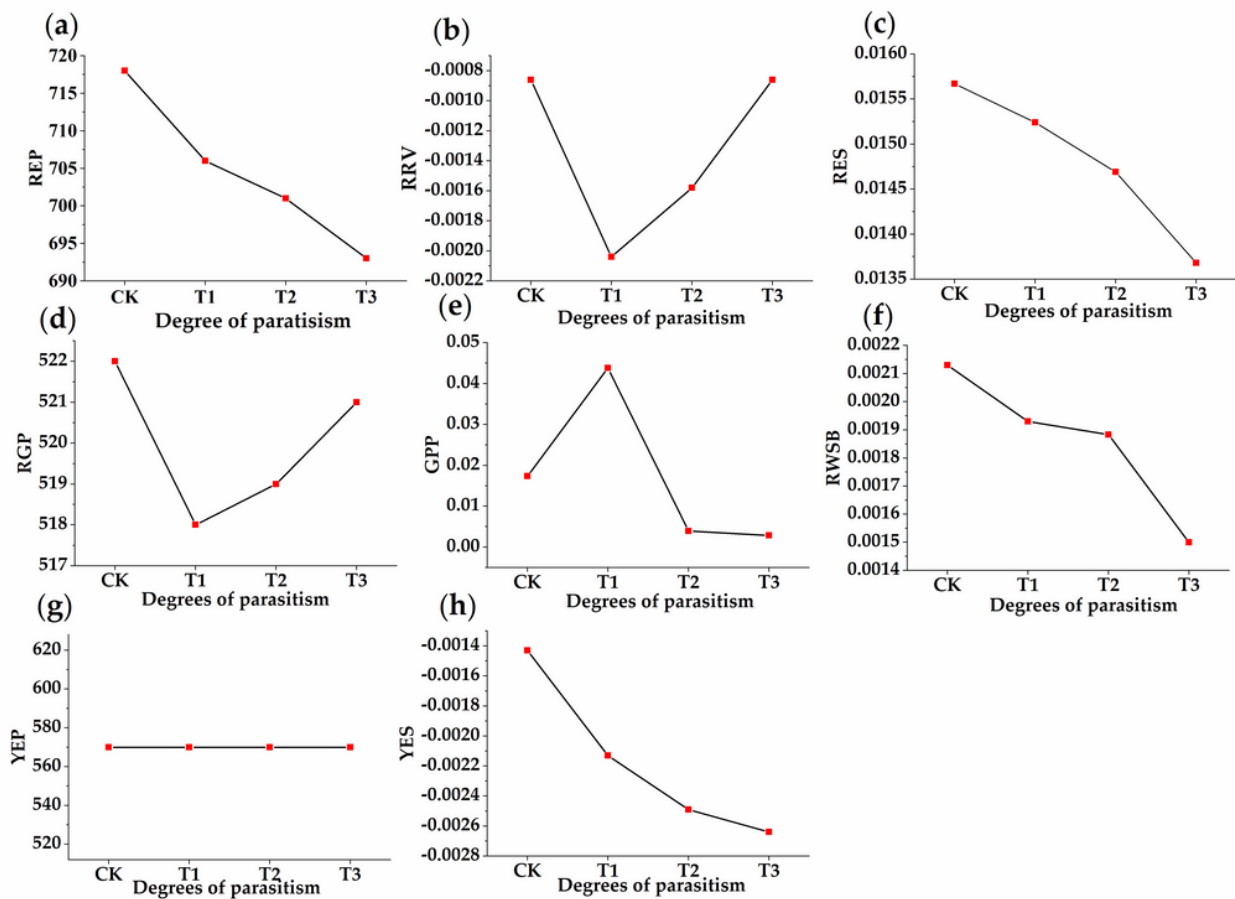


Figure 5

Dynamic trend of spectral parameters in different parasitism period. (a)-(h) respectively represents the position of red edge (REP), the reflectance of red valley (RRV), the slope of red edge (RES), the reflectance of green peak (RGP), the reflection of green peak (GPP), the reflection of water stress band (RWSB), the position of yellow edge (YEP), and the slope yellow edge (YES) under different parasitic intensities.

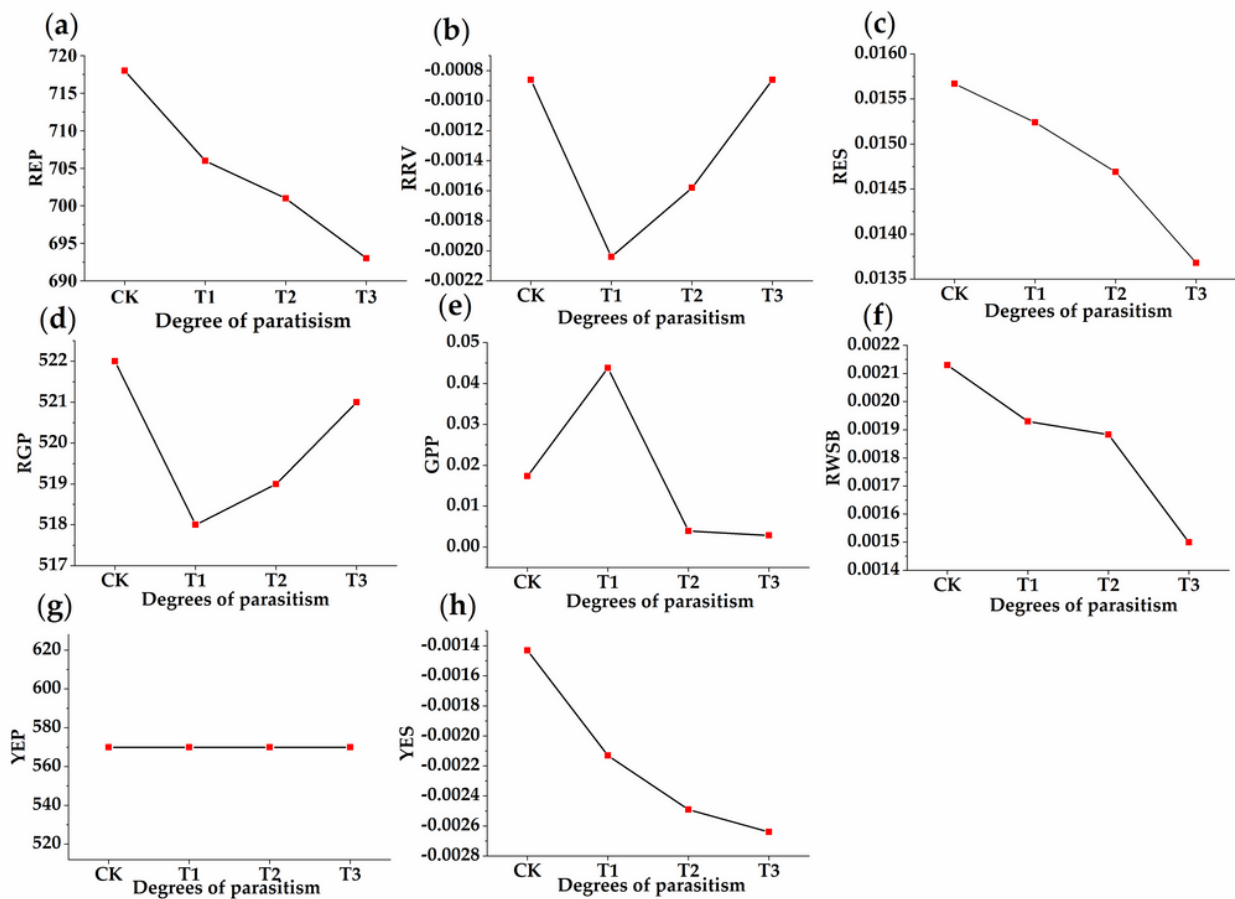


Figure 5

Dynamic trend of spectral parameters in different parasitism period. (a)-(h) respectively represents the position of red edge (REP), the reflectance of red valley (RRV), the slope of red edge (RES), the reflectance of green peak (RGP), the reflection of green peak (GPP), the reflection of water stress band (RWSB), the position of yellow edge (YEP), and the slope yellow edge (YES) under different parasitic intensities.

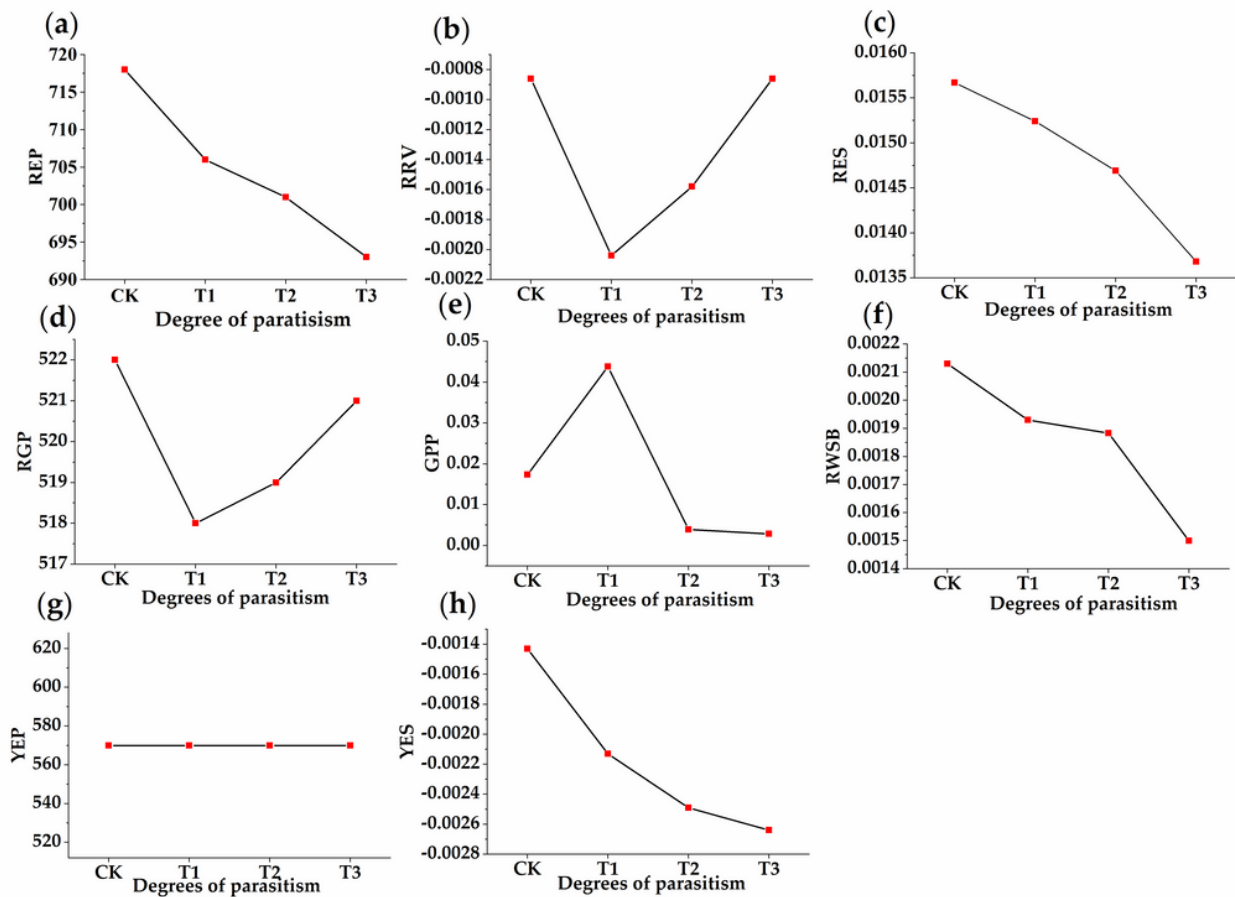


Figure 5

Dynamic trend of spectral parameters in different parasitism period. (a)-(h) respectively represents the position of red edge (REP), the reflectance of red valley (RRV), the slope of red edge (RES), the reflectance of green peak (RGP), the reflection of green peak (GPP), the reflection of water stress band (RWSB), the position of yellow edge (YEP), and the slope yellow edge (YES) under different parasitic intensities.

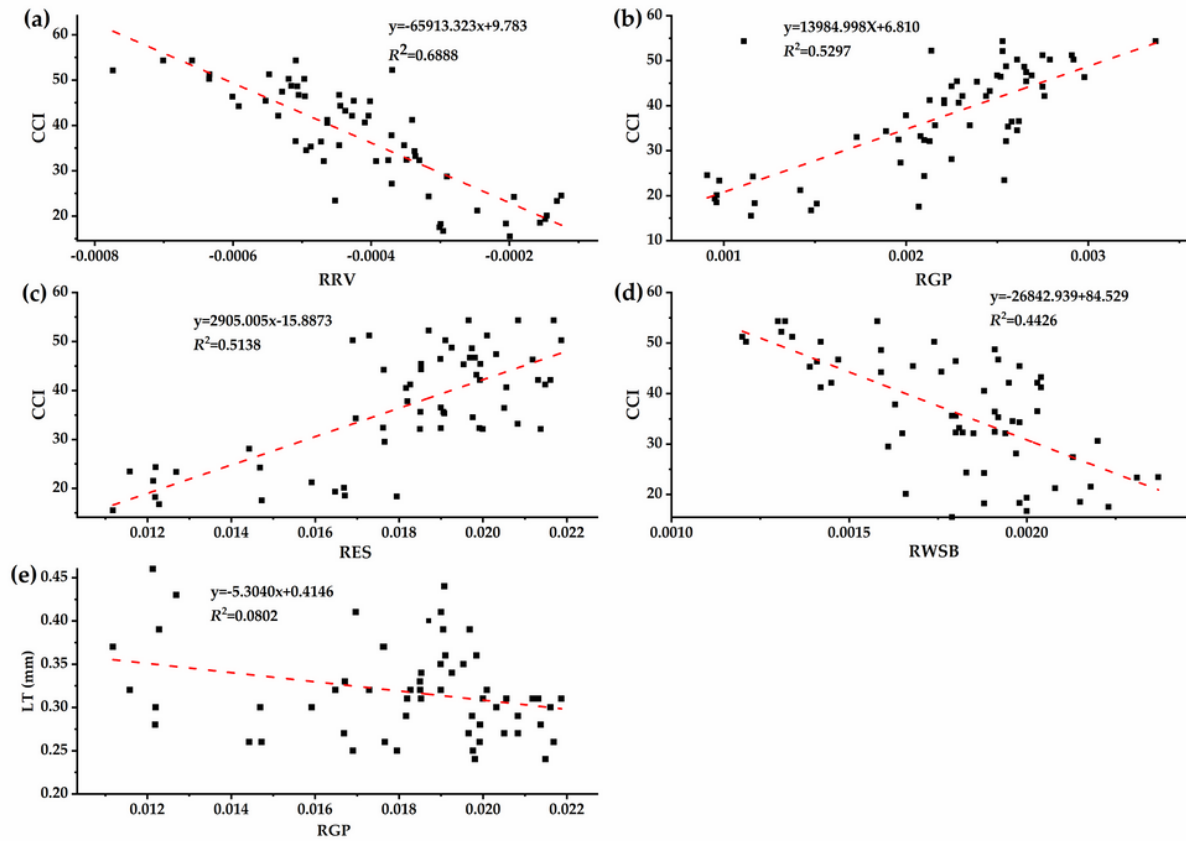


Figure 6

Linear correlation between functional traits and spectral parameters. (a) the reflection of red valley (RRV) and CCI, (b) the reflectance of green peak (RGP) and CCI, (c) the slope of red edge (RES) and CCI, (d) the reflection of water stress band (RWSB) and CCI, (e) the reflectance of green peak (RGP) and LT.

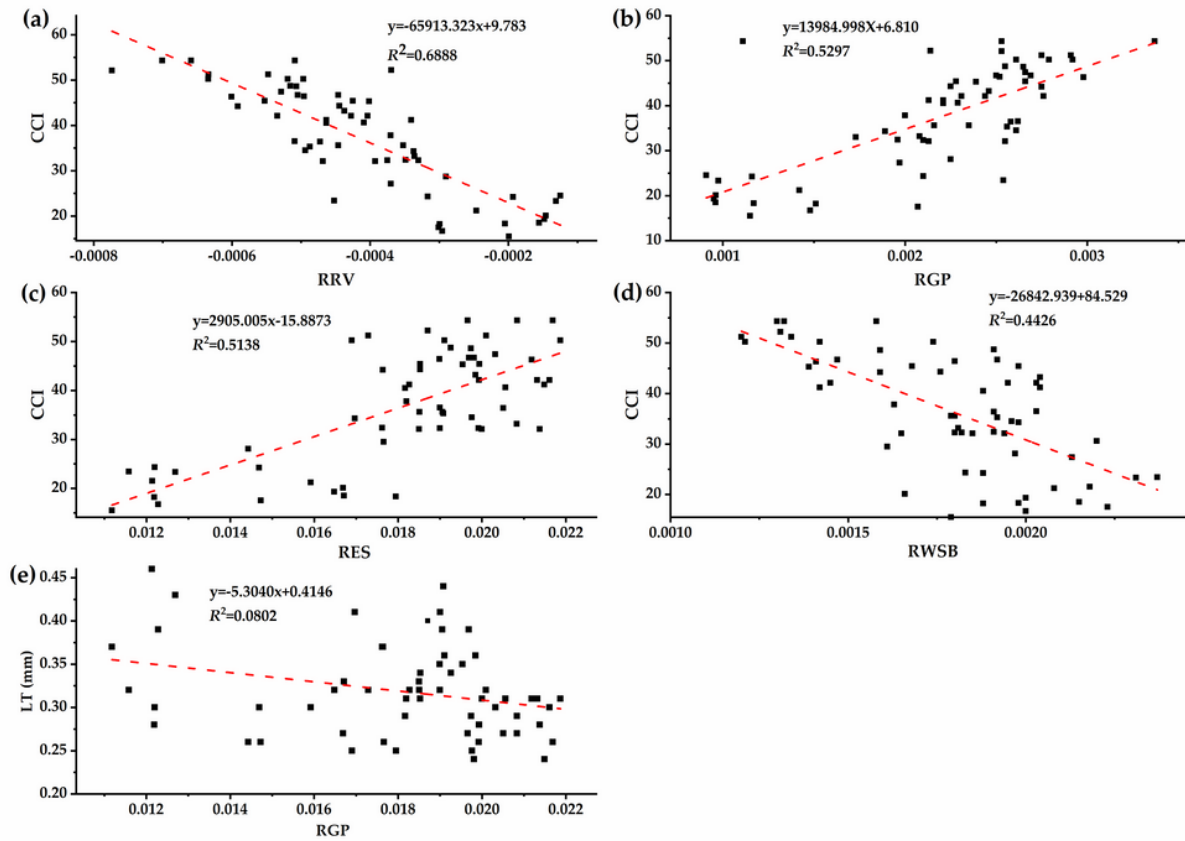


Figure 6

Linear correlation between functional traits and spectral parameters. (a) the reflection of red valley (RRV) and CCI, (b) the reflectance of green peak (RGP) and CCI, (c) the slope of red edge (RES) and CCI, (d) the reflection of water stress band (RWSB) and CCI, (e) the reflectance of green peak (RGP) and LT.

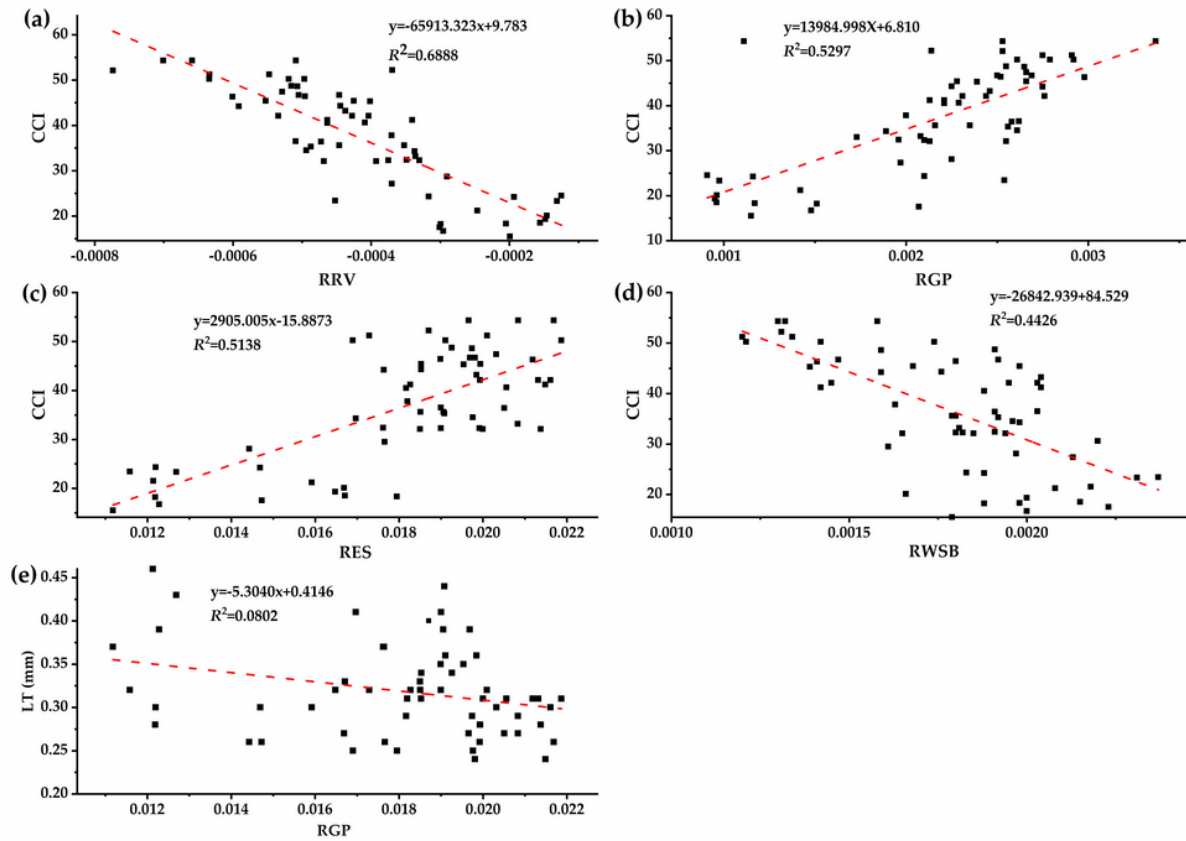


Figure 6

Linear correlation between functional traits and spectral parameters. (a) the reflection of red valley (RRV) and CCI, (b) the reflectance of green peak (RGP) and CCI, (c) the slope of red edge (RES) and CCI, (d) the reflection of water stress band (RWSB) and CCI, (e) the reflectance of green peak (RGP) and LT.

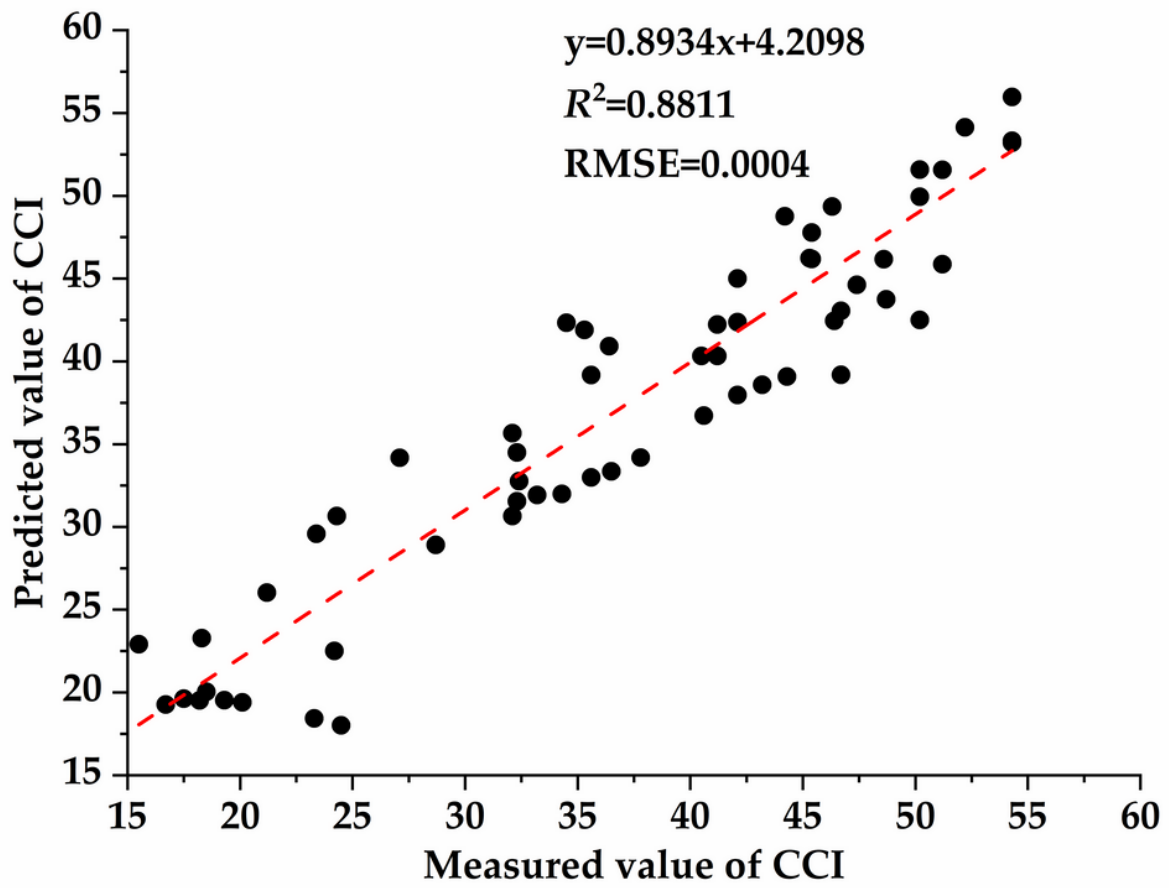


Figure 7

Test of chlorophyll inversion model based on red valley reflectance.

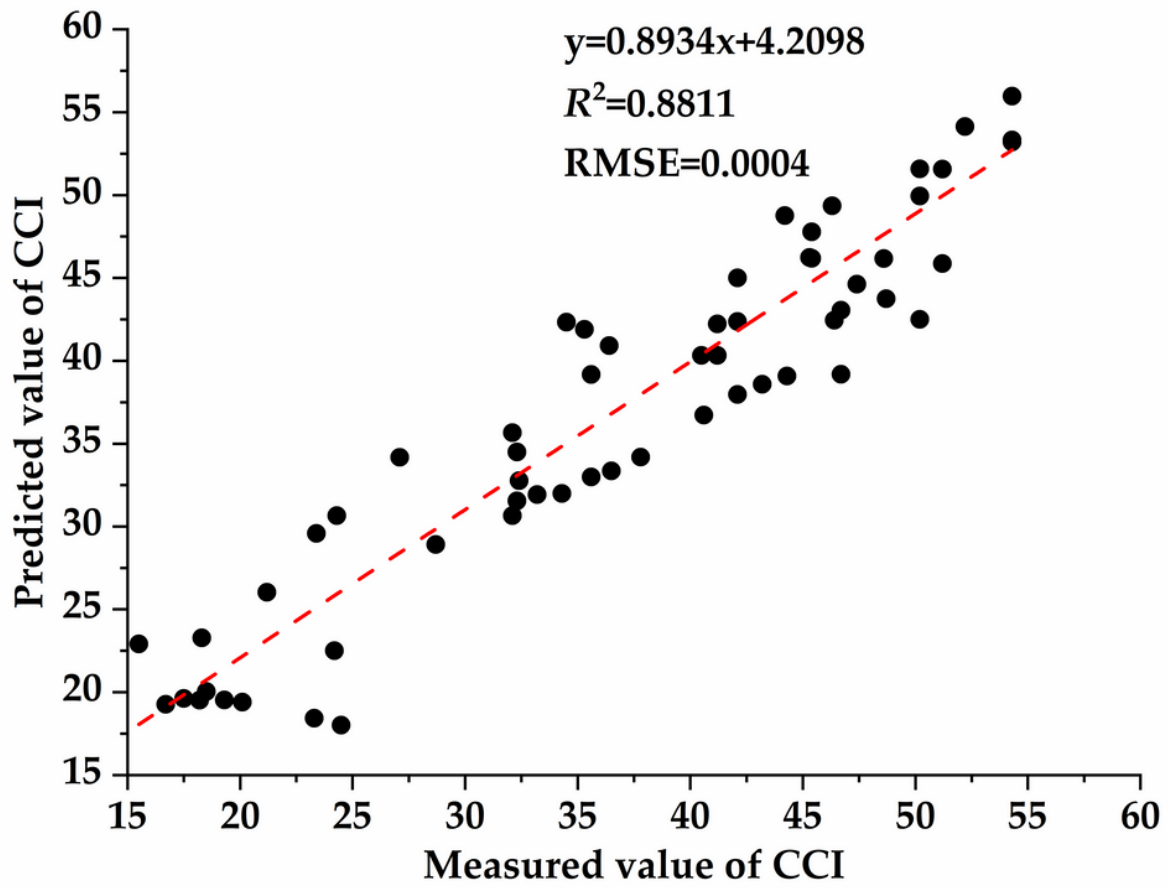


Figure 7

Test of chlorophyll inversion model based on red valley reflectance.

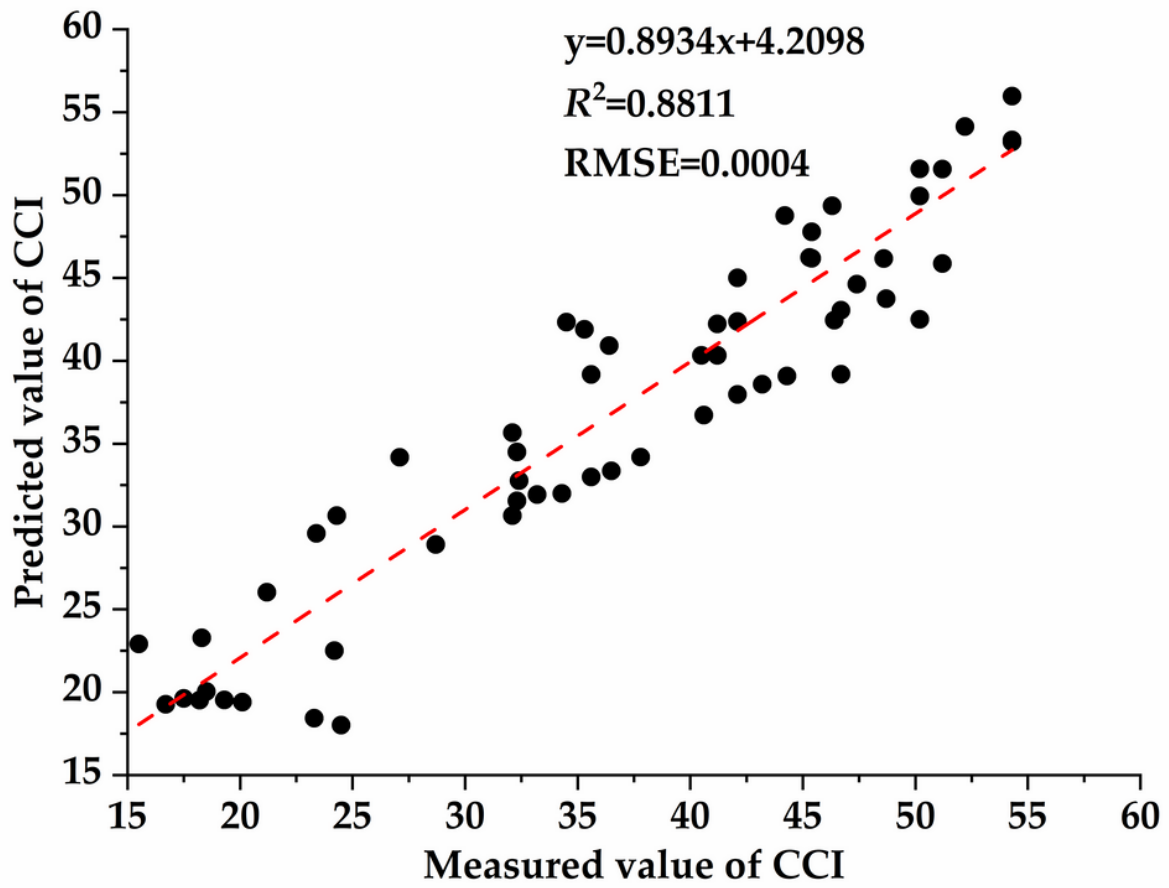


Figure 7

Test of chlorophyll inversion model based on red valley reflectance.

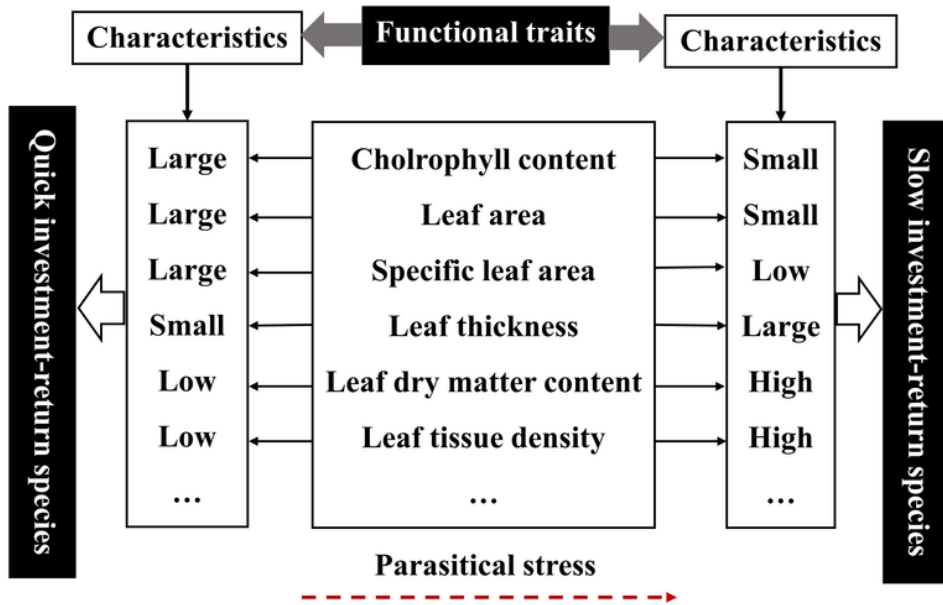


Figure 8

Conceptual illustration of leaf economics spectrum. Quoted from reference Wight et al., 2004.

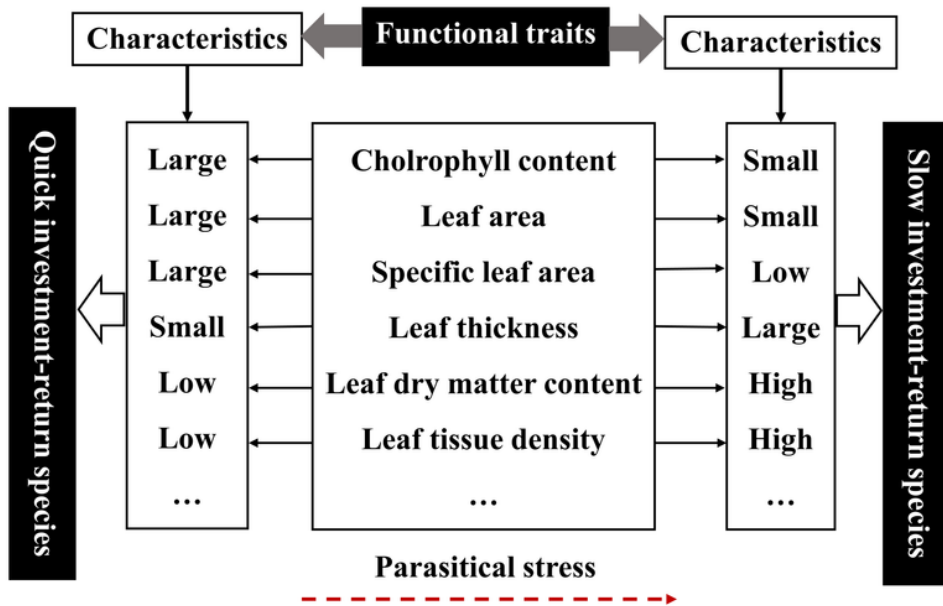


Figure 8

Conceptual illustration of leaf economics spectrum. Quoted from reference Wight et al., 2004.

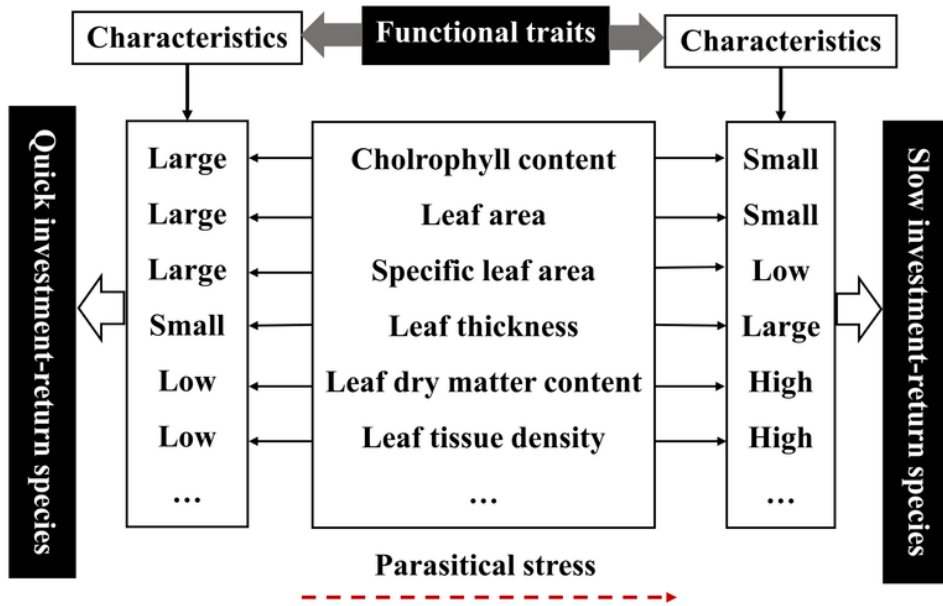


Figure 8

Conceptual illustration of leaf economics spectrum. Quoted from reference Wight et al., 2004.



(a)



(b)

Figure 9

Leaf samples of *Osmanthus fragrans* (Thunb.) Lour. with or without parasitism of *Cuscuta japonica* Choisy. (a) *Osmanthus fragrans* without parasitism of *Cuscuta japonica* Choisy (healthy plant). (b) *Osmanthus fragrans* with parasitism of *Cuscuta japonica* Choisy.



(a)



(b)

Figure 9

Leaf samples of *Osmanthus fragrans* (Thunb.) Lour. with or without parasitism of *Cuscuta japonica* Choisy. (a) *Osmanthus fragrans* without parasitism of *Cuscuta japonica* Choisy (healthy plant). (b) *Osmanthus fragrans* with parasitism of *Cuscuta japonica* Choisy.



(a)



(b)

Figure 9

Leaf samples of *Osmanthus fragrans* (Thunb.) Lour. with or without parasitism of *Cuscuta japonica* Choisy. (a) *Osmanthus fragrans* without parasitism of *Cuscuta japonica* Choisy (healthy plant). (b) *Osmanthus fragrans* with parasitism of *Cuscuta japonica* Choisy.

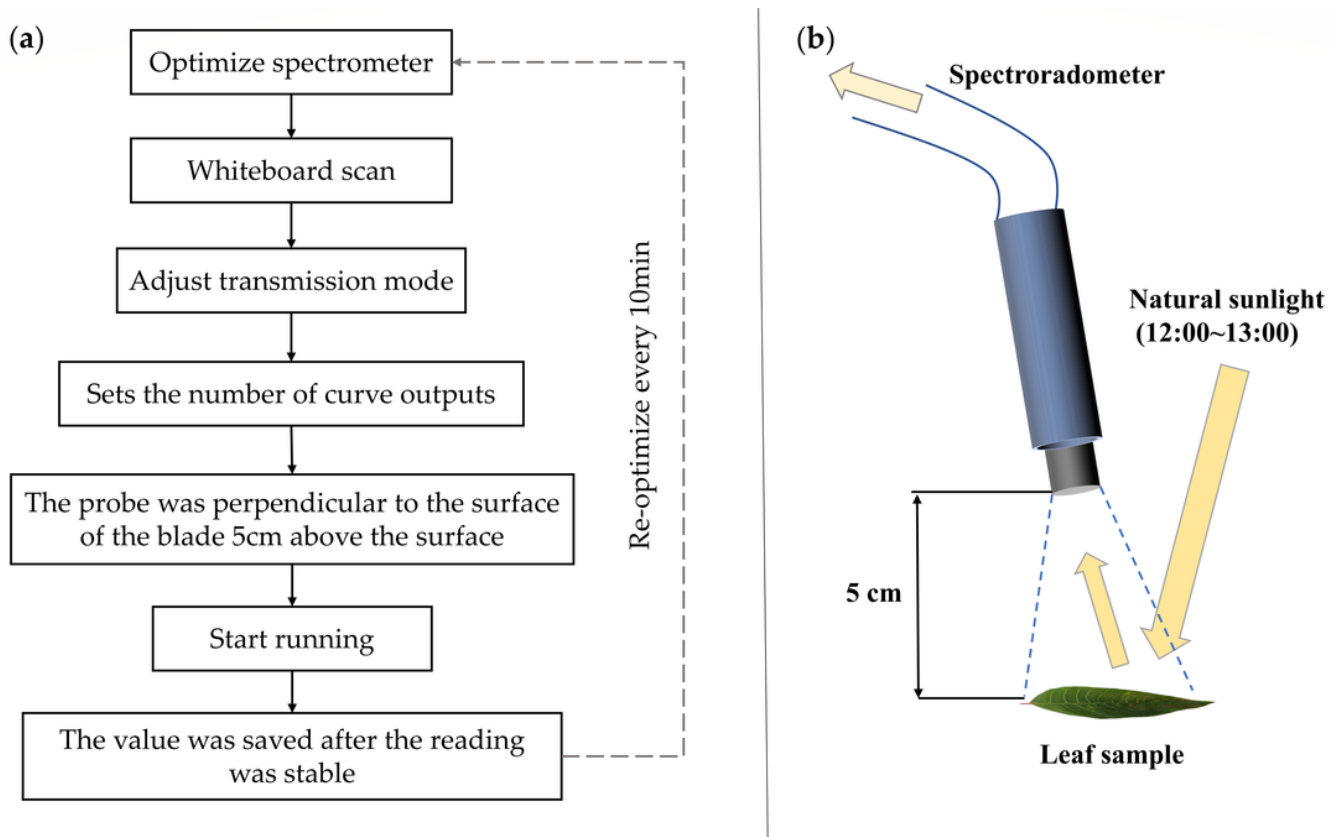


Figure 10

The operation flow of ASD spectrometer for measuring leaf surface spectrum (Quoted from Zhu et al., 2019). (a) is the operation flow of ASD spectrometer. (b) is a schematic diagram of the operation of the spectrometry of the blade.

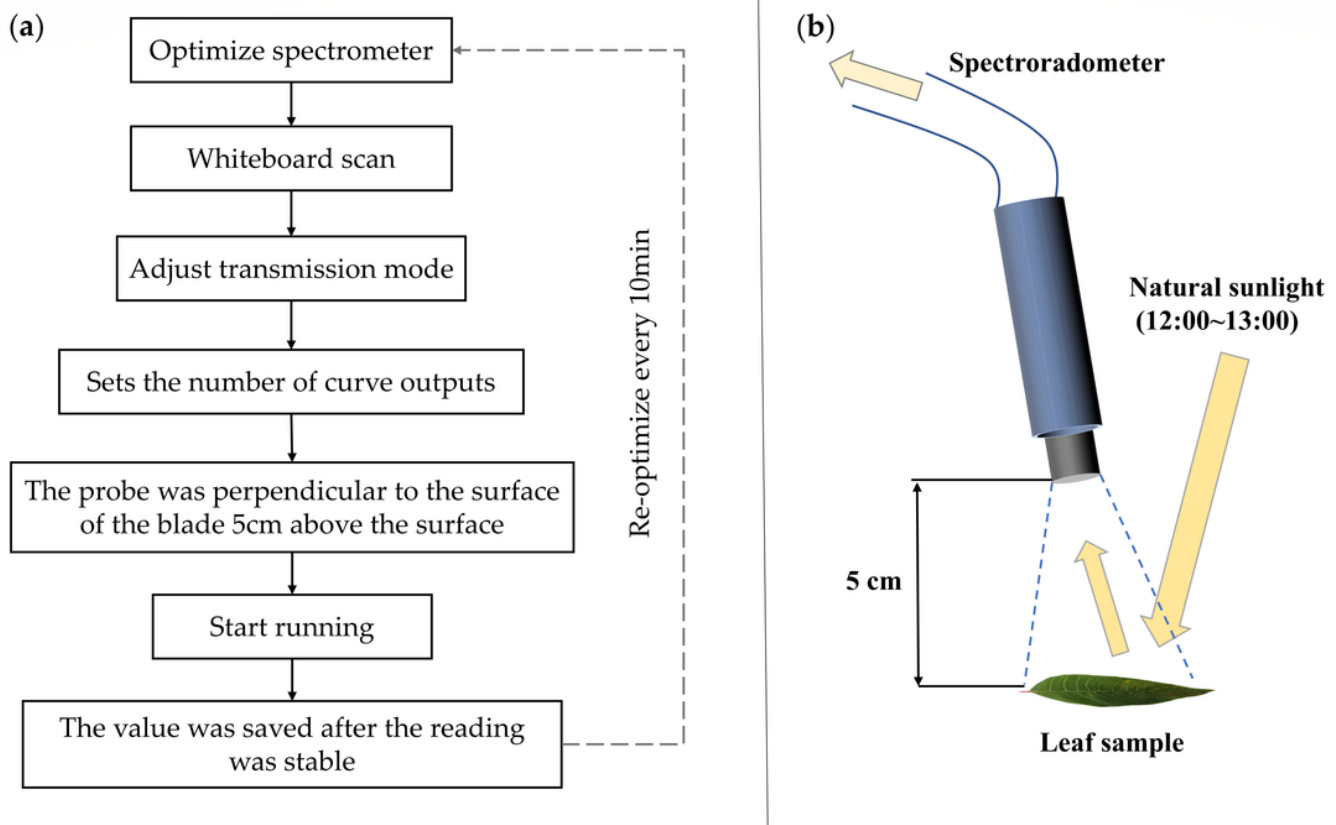


Figure 10

The operation flow of ASD spectrometer for measuring leaf surface spectrum (Quoted from Zhu et al., 2019). (a) is the operation flow of ASD spectrometer. (b) is a schematic diagram of the operation of the spectrometry of the blade.

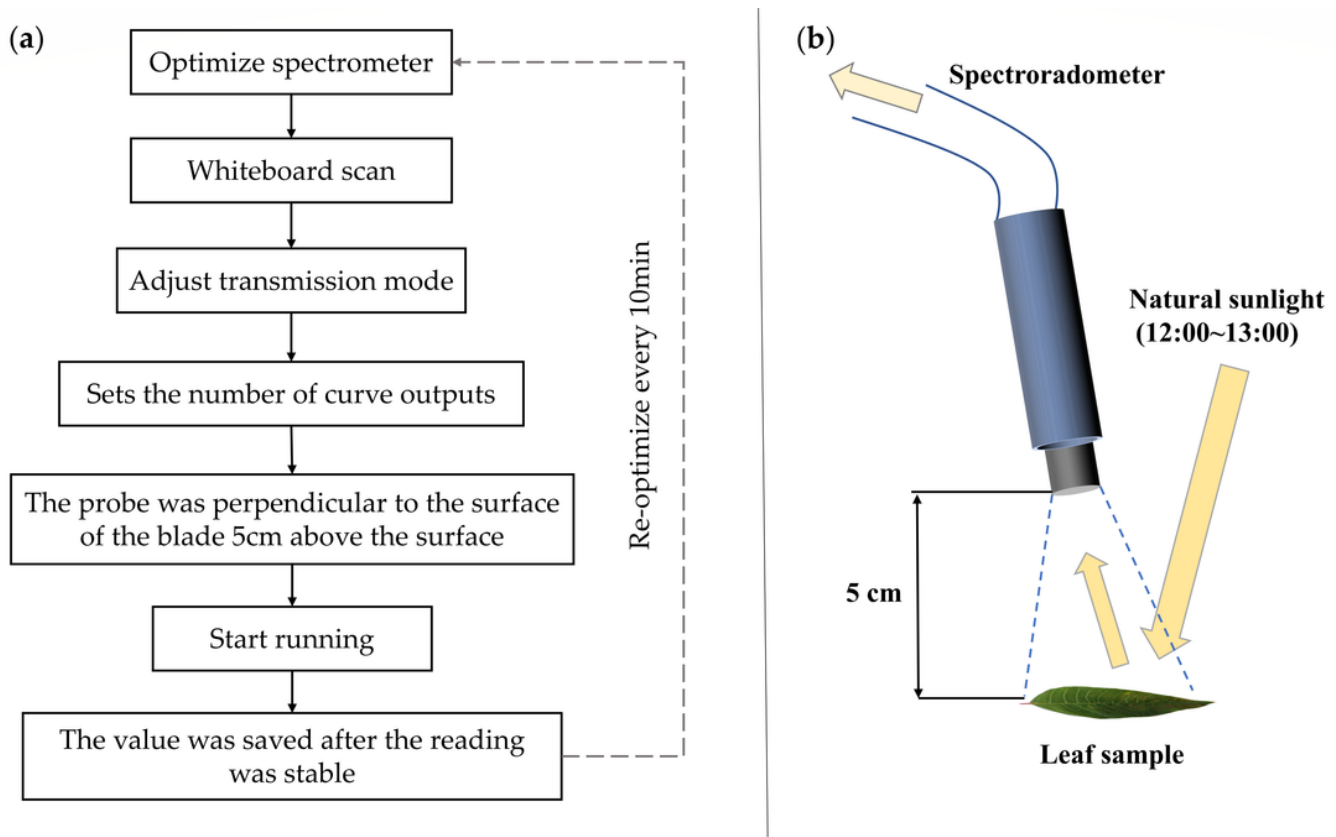


Figure 10

The operation flow of ASD spectrometer for measuring leaf surface spectrum (Quoted from Zhu et al., 2019). (a) is the operation flow of ASD spectrometer. (b) is a schematic diagram of the operation of the spectrometry of the blade.